



**SAVONIA**

THESIS – MASTER'S DEGREE PROGRAMME

TECHNOLOGY, COMMUNICATION AND TRANSPORT

# THERMOELECTRIC GENERATOR

Electricity from Waste Heat

AUTHOR/S:

Matthias Christian Schütt

Field of Study Technology, Communication and Transport	
Degree Programme Master's Degree Programme in Energy Engineering	
Author(s) Matthias Christian Schütt	
Title of Thesis Thermoelectric Generator - Electricity from Waste Heat	
Date 05 December 2022	Pages/Appendices 55 / 9
Client Organization /Partners CTB ceramic technology GmbH Berlin	
<p><b>Abstract</b></p> <p>In this thesis the aim was to study the implementation of thermoelectric generators (TEG) at an industrial kiln system in order to make use of the waste heat during the firing process of ceramics. Besides the need to reduce CO<sub>2</sub> emissions in fossil fuel-fired industrial kilns also new ways to harvest the considerable big amount of waste heat have to be found.</p> <p>Thermoelectric generators convert heat directly into electric energy. They are considerably easy to implement in places where there is excess heat. With the need of generating emission-free energy and rising energy prices, thermoelectric generators could contribute to the energy production mix, despite their low efficiency of up to 5 %.</p> <p>This thesis presents theoretical information about Peltier elements and their use as thermoelectric generators and applications. Besides the theoretical background, an experimental setup was conducted to find out the performance of the thermoelectric generators and observe in practice the considerations to be made when designing and implementing TEGs.</p> <p>The possible implementation of TEG into a kiln system was analyzed based on a reference kiln. In addition to calculations of electrical energy output suggestions for design approaches were made to optimize implementation. Also, an estimate of investment cost was made to answer the question whether it is economically beneficial to install a thermoelectric generator or not.</p> <p>As a result, it can be said that the implementation of thermoelectric generators into a kiln system can be, despite the low efficiency, quite useful. Especially with drastically increasing energy it can be a competitive way of producing electrical energy. The experimental setup showed the importance careful design, especially for maintaining a good heat dissipation.</p>	
<p><b>Keywords</b> Thermoelectric Generator, TEG, Seebeck effect, Peltier element, CTB ceramic technology</p>	

Koulutusala Tekniikan ja liikenteen ala	
Tutkinto-ohjelma Master's Degree Programme in Energy Engineering	
Työn tekijä(t) Matthias Christian Schütt	
Työn nimi Thermoelectric Generator - Electricity from Waste Heat	
Päiväys 5. joulukuuta 2022	Sivumäärä/Liitteet 55 / 9
Toimeksiantaja/Yhteistyökumppani(t) CTB ceramic technology GmbH Berlin	
Tiivistelmä	
<p>Tässä opinnäytetyössä tutkitaan termoelektristä generaattoria (TEG) käyttöönottoa teollisuus-uunissa hukkalämmön hyödyntämiseksi keramiikan polttoprosessin aikana. Fossiilisia polttoaineita käyttävän teollisuusuunin hiilidioksidipäästöjen vähentämisen lisäksi on löydettävä uusia tapoja kerätä huomattava määrä hukkalämpöä.</p> <p>Lämpösähkögeneraattorit muuntavat lämmön suoraan sähköenergiaksi. Ne ovat huomattavan helppo toteuttaa paikoissa, joissa esiintyy ylimääräistä lämpöä. Kun tarvitaan päästötöntä energiaa, huomioonottaen energian hintojen nousu, lämpösähkögeneraattorit voisivat vaikuttaa kokonaisenergiantuotantoon, vaikka niiden tehokkuus on vain alle 5 prosenttia.</p> <p>Opinnäytetyössä esitetään teoreettista tietoa Peltier-elementeistä, joita käytetään lämpösähköisinä generaattoreina ja -sovelluksina. Teoreettisen taustan lisäksi tehtiin kokeellinen asennus lämpösähkögeneraattorin suorituskyvyn tutkimiseksi ja havainnoimiseksi käytännössä, mitä pitää huomioida kun suunnitellaan ja otetaan käyttöön TEG: ta.</p> <p>Lämpösähkögeneraattorin mahdollista käyttöönottoa teollisuusuunijärjestelmässä analysoitiin testiuunin perusteella. Sähköenergian tuotosehdotusten lisäksi tehtiin ehdotuksia suunnitteluun ja toteutuksen optimointiin. Arvioitiin investointikustannukset, jotta voidaan vastata kysymykseen siitä, onko lämpösähkögeneraattorin asentaminen taloudellisesti hyödyllistä vai ei.</p> <p>Tämän seurauksena voidaan sanoa, että lämpösähköisten generaattoreiden toteuttaminen uunijärjestelmään voi olla alhaisesta hyötysuhteesta huolimatta varsin hyödyllistä. Varsinkin rajusti kohonneiden sähköenergian hintojen myötä se voi olla kilpailukykyinen tapa tuottaa sähköenergiaa. Kokeellinen järjestely osoitti huolellisen suunnittelun tärkeyden erityisesti hyvän lämmönpoiston ylläpitämiseksi.</p>	
Avainsanat termoelektrik generaattori, TEG, Seebeck-vaikutus, Peltier-elementti, CTB ceramic technology	

## CONTENTS

1	INTRODUCTION .....	9
1.1	CTB ceramic technology GmbH Berlin .....	9
2	THERMOELECTRICITY .....	10
2.1	Seebeck effect .....	10
2.1.1	Principal of the Seebeck effect .....	11
2.1.2	Seebeck Coefficient .....	12
2.1.3	Thermocouple .....	13
2.2	Peltier effect .....	14
2.3	Thomson effect .....	15
2.4	Joule heating .....	16
3	THERMOELECTRIC GENERATOR .....	17
3.1	Carnot efficiency .....	17
3.2	Working principle of TEG .....	18
3.3	Structure of the TEG .....	20
3.4	Semiconductor .....	21
3.5	TEG design approaches .....	22
3.6	Output voltage and current .....	24
3.7	Electrical Power .....	25
3.8	Heat supply, heat removal and heat development .....	26
3.9	Cooling off thermoelectric generators .....	28
3.9.1	Natural convectional cooling .....	28
3.9.2	Forced convectional cooling .....	28
3.9.3	Liquid cooling .....	28
3.10	Efficiency .....	29
3.10.1	Efficiency calculation .....	30
3.11	TEG operating conditions .....	31
3.11.1	Temperatures .....	31
3.11.2	Vibrations .....	31
3.11.3	Corrosion .....	31
3.11.4	Fastening of the TEG .....	32
3.11.5	Lifespan .....	32
3.12	Future of TEG .....	33

4	EXPERIMENTAL SETUP .....	34
4.1	Mounting.....	36
4.1.1	Stack effect .....	36
4.2	Heat source.....	37
4.3	Electrical connection .....	38
4.4	Theoretical electrical output power .....	39
4.5	Conclusion of the experimental setup.....	40
5	POTENTIAL THERMOELECTRIC GENERATOR SETUP FOR A KILN .....	42
5.1	Reference Kiln .....	42
5.2	Forced cooling of Peltier elements.....	43
5.3	TEG outline .....	44
5.3.1	Choice of TEG module .....	45
5.3.2	Heat sink dimensioning.....	48
5.3.3	Electrical output power .....	50
5.4	Costs analyzes .....	50
6	DISCUSSION .....	52
	REFERENCES .....	53
	APPENDIX 1: DATASHEET TEC1-12706 .....	56
	APPENDIX 2: DC-DC CONVERTER .....	59
	APPENDIX 3: PELTIER ELEMENT MANUFACTURES .....	61
	APPENDIX 4: DATASHEET TEC2H-50-50-207/68 .....	62
	APPENDIX 5: HEAT SINK.....	63
	APPENDIX 6: EXAMPLE OF A BELL KILN .....	64

## LIST OF FIGURES AND TABLES

Figure 1. Thomas Johann Seebeck .....	10
Figure 2. Seebeck's experimental setup for connecting bismuth (B) and copper (K).....	10
Figure 3. Temperature difference creates an electrical potential .....	11
Figure 4. Principle of the Seebeck effect .....	11
Figure 5. Thermocouple.....	14
Figure 6. Peltier effect (left) as opposed to the Seebeck effect (right) .....	15
Figure 7. Thermoelectric effects .....	15
Figure 8. Principle of Carnot efficiency .....	17
Figure 9. Typical TEG: (a) Basic principle, (b) Equivalent electrical circuit .....	18
Figure 10. Self-portrait of NASA's Curiosity Mars rover .....	20
Figure 11. TEC Module type TEC1-12706 .....	20
Figure 12. Schematic of a commercial thermoelectric generator module .....	21
Figure 13. Schematic representation of p-doping (left) an n-doping (right) .....	22
Figure 14. Planar TEG design .....	23
Figure 15. Vertical TEG design .....	23
Figure 16. Mixed TEG design.....	24
Figure 17. Multistage thermoelectric generator .....	24
Figure 18. Types of heat at a TEG.....	27
Figure 19. Thermoelectric generator output .....	29
Figure 20. TEG Efficiency vs. temperature differences .....	30
Figure 21. Attenuation with elastic thermal adhesive .....	31
Figure 22. Design model of the Exhaust stack .....	34
Figure 23. Experimental Setup .....	35
Figure 24. Heat sink .....	36
Figure 25. AGIA TEX thermal adhesive .....	36
Figure 26. Principle of the stack effect.....	37
Figure 27. TEG electrical connection.....	39
Figure 28. Output voltage of TEG.....	41
Figure 29. Exhaust stack.....	44
Figure 30. rectangle shaped exhaust stack .....	45
Figure 31. Fastening of TEG.....	46
Figure 32. Peltier element with centered hole .....	47

Table 1. Seebeck coefficient of materials .....	12
Table 2. Voltage Change vs. Temperature Rise for Various thermocouple types at 25°C .....	14
Table 3. Measured internal resistance of Peltier elements .....	38
Table 4. Thermal and electrical data of Peltier element.....	47
Table 5. Volumetric Thermal resistance of air.....	48
Table 6. Fin Spacing versus Flow and Fin Length .....	49

## LIST OF ABBREVIATIONS

A	ampere
C	Celsius
$E$	electric field strength
I	current
$j$	current density
$J_c$	current flow direction
K	Kelvin
$L$	arm length of the thermocouples crossed by the heat flow
M	meter
P	power
POC	product of combustion
Q	Joule heating
$Q_{in}$	input energy
$Q_{wl}$	heat conduction
$\dot{q}$	heat flux density
$R_L$	load resistance
$R_{TEG}$	internal resistance of thermoelectric generator
Rv	volumetric thermal resistance of the air
S	siemens
$S$	cross-sectional area of the thermocouples
T	temperature
TC	thermocouple
TEG	thermoelectric generator
TO	thermal oxidizer
U	voltage
$U_{th}$	thermoelectric voltage
V	volt
$V_{out}$	output voltage
VOC	volatile organic compounds
W	Watt
$W_{out}$	mechanical output work
ZT	figure of merit
$\alpha$	Seebeck coefficient [mV/K]
$\beta_{wl}$	thermal conductivity [W / K]
$\Delta T$	temperature difference
$\eta$	efficiency
$\lambda$	thermal conductivity [W/(m*K)]
$\rho$	electrical resistivity of material
$\sigma$	electric conductivity [S/m]

## 1 INTRODUCTION

The industry for thermal treatment of materials is by nature consuming much energy, mostly by combustion of fossil fuels, which is converted into heat. This heat is necessary to process materials like steel, cement, glass and ceramics. Many efforts had been implemented to recover heat from the thermal process, such as the implementation of heat exchangers. But even in a highly sophisticated installation a considerable large amount of thermal energy is discharged into the air. Making use of this thermal energy, otherwise wasted, has the potential to increase the efficiency of thermal processing machinery and thus contribute to the climate protection by reducing greenhouse gas emissions.

This project aimed to investigate the implementation of thermoelectric generators (TEG) into the exhaust system of an industrial kiln as one part of waste heat recovery. The use of exhaust heat is becoming more and more important in the firing industry. The use of heat exchangers and exhaust gas recovery is already standard for many kiln designs. They have become an essential part of a well-designed kiln. The radiated heat from the flue gas duct, even it is well isolated, is usually just emitted to the ambient and not utilized, except to heat the ambient air. Thermoelectric generators can make use of the heat radiated from the exhaust system by converting the waste heat directly into electricity.

The focus of this work is to find possible solutions and assess the usefulness in the sense of engineering effort and cost-benefit relation. In other words, make a feasibility study.

With the ongoing climate change and therefore the need to reduce greenhouse gas emissions by designing more energy-efficient kilns, the integration of thermoelectric generators could be an additional feature to the system to make use of waste heat, which would be otherwise difficult to harvest.

### 1.1 CTB ceramic technology GmbH Berlin

CTB ceramic technology GmbH Berlin is a small innovative company based in Berlin, which is specialized to design, build and install kilns for all thermal processes in the ceramics industry with temperatures up to 1800 °C as well as for research and development purposes. In its over 27 years of successful operating business, it has a proud history of realizing many projects from small research kilns to very large production kilns for the car industry. The company is working closely together with its customer to find very specific solutions that match the special needs of the customer. CTB is always keen to develop a custom firing solution. Besides the construction of new facilities, the company is also handling modernizations to meet new standards and regulations of older kilns, which also helps to save energy costs. To the company's service belong also feasibility studies and firing simulations.

## 2 THERMOELECTRICITY

A short definition for thermoelectricity is, that it describes the direct conversion of a temperature gradient into electricity and vice versa. There are three thermoelectric effects. The Seebeck effect, the Peltier effect, and the Thomson effect.

### 2.1 Seebeck effect

The actual function of a thermoelectric generator is based on the Seebeck effect. The name was given after its discoverer, the German physician and physicist, Thomas Johann Seebeck (Figure 1), who was born April 9th, 1770 in Reval (today Tallinn) and died December 10<sup>th</sup>, 1831 in Berlin.



Figure 1. Thomas Johann Seebeck (Browse Biography, 2010)

The discovery was made in 1821 while experimenting with different materials. He connected two different metals, bismuth and antimony, to copper. The materials were mounted in the form of discs on one terminal of a spiral copper wire in whose center a compass was placed (Figure 2). He observed a deflection of the needle. The deflection of the compass needle in the case of antimony was opposite to that in the case of bismuth. (Fahrner & Schwertheim, 2009)

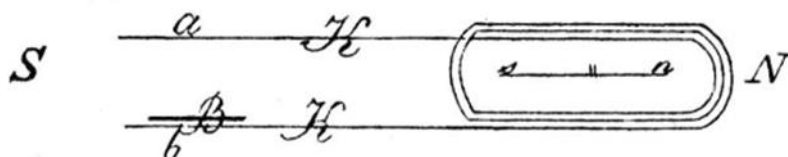


Figure 2. Seebeck's experimental setup for connecting bismuth (B) and copper (K) (Seebeck, 1895)

Seebeck initially believed that it was due to the magnetism induced by the temperature differences and he called the effect a thermo-magnetic effect. However, Danish physicist, Hans Christian Orsted realized that it is an electrical current that is induced, which because of Ampere law deflects the magnet. (Electrical 4 U, 2020)

### 2.1.1 Principal of the Seebeck effect

The Seebeck effect can be observed by heating up a piece of conducting material, e.g., a copper rod on one end and leaving the other at room temperature. Because of the temperature difference between each end of the copper rod the electrons also move at different speeds and therefore have a different kinetic energy. The electrons on the hot side move with higher speed and thus need more space. This electromotive force of the electrons pushes back the electrons from the colder side. This leads to a more negative charge at the colder end than the warmer end, due to the inhomogeneous distribution of the electrons in the copper rod. See Figure 3.

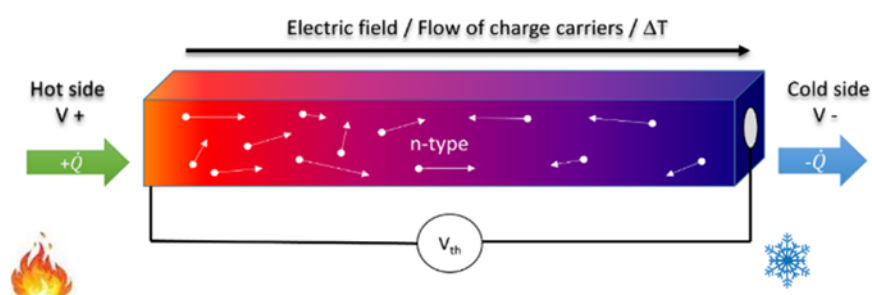


Figure 3. Temperature difference creates an electrical potential (Linseis, 2021)

If now two different conducting materials, such as metal or semiconductor, are connected in parallel through an electrical circuit like in Figure 4 the same phenomena occur. The electrons from the hot side  $T_H$  flow to the colder side  $T_C$ , meaning the electrons with higher energy flow into the direction of the electrons with lower energy and vice versa. Only that the conducting materials have a different atomic lattice construction and free electrons which create together with temperature difference an electrical potential between the connecting points. This potential difference is proportional to the temperature difference. Having a closed-loop circuit, an electric current is flowing and thus a Seebeck voltage or thermoelectric voltage is present.

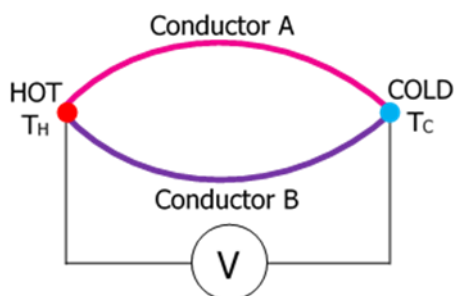


Figure 4. Principle of the Seebeck effect (Electrical for Us, 2016)

The amount of voltage produced is, as seen in Equation (1) for the thermoelectric voltage  $U_{th}$  [V], directly dependent on the difference in temperature between two junction points, the hot junction point and the cold junction point as well as in the difference of the Seebeck coefficient of two different conducting materials connected to each other.

$$U_{th} = (\alpha_1 - \alpha_2) * (T_H - T_C) \quad (1)$$

where,

$\alpha_1$  and  $\alpha_2$  = Seebeck coefficient of conductor A and B (Schröter, 2008)

### 2.1.2 Seebeck Coefficient

The Seebeck coefficient, also called thermoelectric power or thermoelectric sensitivity, of a material measures the magnitude of and induced thermoelectric voltage in response to a temperature difference across that material. It has the dimensions of V/K. See Equation (2).

$$\alpha = \frac{-U_{th}}{\Delta T} \quad (2)$$

where,

$\alpha$  = Seebeck coefficient [V/K]

$U_{th}$  = thermoelectric Voltage [V]

$\Delta T$  = Temperature difference [K]

The Seebeck coefficient is not entirely linear, it varies at different temperatures. This is important for certain temperature ranges and thermoelectric measurement technology. Some examples of the thermoelectric series with their thermoelectric effects, Seebeck coefficients and the associated thermal conductivity values are listed in Table 1.

Table 1. Seebeck coefficient of materials (Schröter, 2008)

material		Seebeck-coefficient $\alpha$ [mV/K]	Thermal conductivity $\lambda$ [W/(m*K)]
Fe	iron	1,7	72
Cu	copper	0,7	398
Ag	silver	0,65	418
Al	aluminum	0,4	238
Pt	platinum	0	71
Ni	nickel	-1,5	61
Bi	bismuth	-7,3	8,1
W	tungsten	0,7	130
Si	silicon	45	80
Bi <sub>2</sub> Te <sub>3</sub>	bismuth- telluride		1,2
	(n-doped)	-287	
	(p-doped)	81	
B <sub>13</sub> C <sub>2</sub>	aluminum doped boron carbide	440	0,02

A Seebeck-element always consists of two different conducting materials, the material properties must be summarized in one element parameter. In the electrical series connection of resistances, these are added and thus the conductance, which represents the reciprocal value, is subtracted. Since the thermal voltage occurs only through the potential difference in the pair of legs  $\alpha_1$  and  $\alpha_2$  [V/K] they must be subtracted from each to become  $\alpha$ . The same analogy can be applied to the thermal conductivity. Thus  $\sigma_1$  and  $\sigma_2$  [S/m], become  $\sigma$ . The thermal conductivity  $\lambda_1$  and  $\lambda_2$  [W/(m\*K)] are subtracted to form  $\lambda$ . In addition to the conditions for the thermoelectric voltage, the conductivity and thermal conductivity play important roles, see Equation (4) for the efficiency. The electric conductivity  $\sigma$  [S/m], the reciprocal value of electrical resistance  $\rho$  [ $\Omega$  m], should be high and the thermal conductivity  $\lambda$  [W/(m\*K)] must be low to get a good *figure of merit*,  $Z$ , which describes the performance of a thermoelectric device. Its unit is  $1/^\circ\text{C}$  for the material. However, good electrical conductivity of the material also means good thermal conductivity. As can be seen, this thermal conductivity reduces the *figure of merit* and thus the possible degree of efficiency. Since the Seebeck coefficient in Equation (3) is square, it forms the part of the Equation which should be optimized the most. (Schröter, 2008)

$$Z = \frac{\alpha^2 * \sigma}{\lambda} \quad (3)$$

where,

$\alpha$  = summarized Seebeck coefficient of both materials

$\sigma$  = electric conductivity

$\lambda$  = thermal conductivity

Equation (4) shows the efficiency of a Seebeck-element.

$$\eta = \frac{T_H - T_C * \left( \sqrt{1 + \frac{\alpha^2 * \sigma * Z}{\lambda} * (T_H - T_C)} - 1 \right)}{T_H - T_C * \sqrt{1 + \frac{\alpha^2 * \sigma * Z}{\lambda} * (T_H - T_C)}} \quad (4)$$

### 2.1.3 Thermocouple

A thermocouple, in short TC, is probably the most known measuring device using the phenomenon of the thermoelectric effect. The thermocouple directly converts temperature differences to an electric voltage. The electrical voltage that occurs at the ends of the metallic conductors is comparatively small and is, depending on the conducting materials, in the range of a few  $10 \mu\text{V}$  per  $1^\circ\text{C}$  temperature difference. Table 2 shows the change of voltage with rising temperature of some common thermocouple types. Note that the voltage signal is nonlinear. The slope of a thermocouple response curve changes over temperature. For example, at  $0^\circ\text{C}$  a T-type thermocouple output changes at  $39 \mu\text{V}/^\circ\text{C}$ , but at  $100^\circ\text{C}$ , the slope increases to  $47 \mu\text{V}/^\circ\text{C}$ . (Matthew & Towey, 2010)

Table 2. Voltage Change vs. Temperature Rise for Various thermocouple types at 25°C. (Matthew & Towey, 2010)

thermocouple type	Seebeck-coefficient [ $\mu\text{V}/^\circ\text{C}$ ]
E	61
J	52
K	41
N	27
R	9
S	6
T	41

Thermocouples have become the industry-standard method for cost-effective measurement of a wide range of temperatures with reasonable accuracy. They are used in a variety of applications up to approximately +2500 °C. The most popular thermocouple is the type K, consisting of Chromel<sup>®</sup> and Alumel<sup>®</sup> (trademarked nickel alloys containing chromium, and aluminum, manganese, and silicon, respectively), with a measurement range of -200 °C to +1250 °C. (Matthew & Towey, 2010) Figure 5 shows the working principle of a thermocouple.

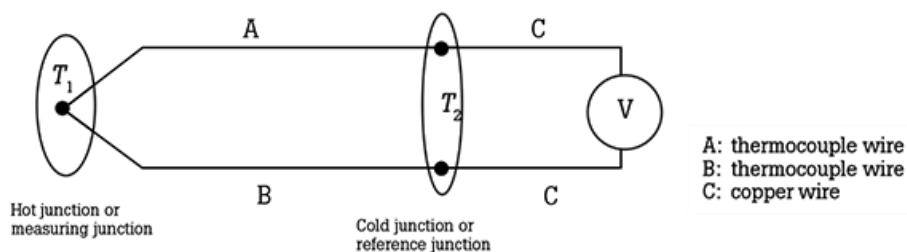


Figure 5. Thermocouple (Fluke, 2021)

## 2.2 Peltier effect

The Peltier effect is basically the opposite principle of the Seebeck effect. The flow of an electrical current through the junction connecting two different conducting materials causes the cooling of one junction while heating the other. This was discovered by Jean Peltier, a watchmaker born February 22nd 1785 in Ham (France), who experimented with electrodynamics. He died on October 27th 1845, in Paris.

The effect is used in Peltier elements, which work like a heat pump. The most common applications are hotel refrigerators, since they are silent and portable cooling boxes because of their compact and small design. Figure 6 shows a comparison of the Seebeck effect and the Peltier effect as function diagram.

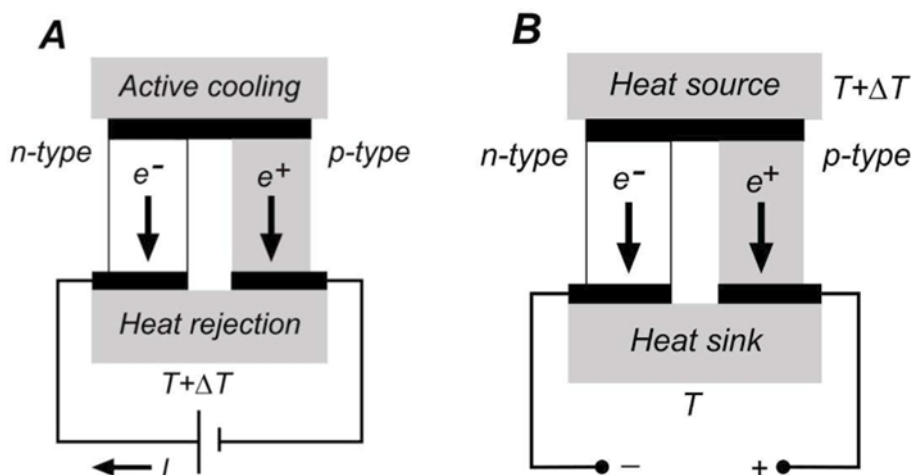


Figure 6. Peltier effect (left) as opposed to the Seebeck effect (right) (Fahrner & Schwertheim, 2009)

### 2.3 Thomson effect

This Thomson effect was predicted in 1851 and later observed by Professor William Thomson (later known as Lord Kelvin). It describes that if a temperature difference exists between any two points of a current-carrying conductor, heat is either absorbed or liberated depending on the direction of current and material (Western Michigan University, 2020). There is also another form of heat, called *Joule heating*, which is irreversible and is always generated as current flows in a wire. The Thomson heat is reversible between heat and electricity. This heat is not the same as Joule heating, seen in Equation (6). (Lee H. S., 2010) Figure 7 shows all three thermoelectric effects, where the Thomson effect is on the right side, comparing that the heat is either absorbed or liberated, depending on the current ( $J_c$ ) flow direction.

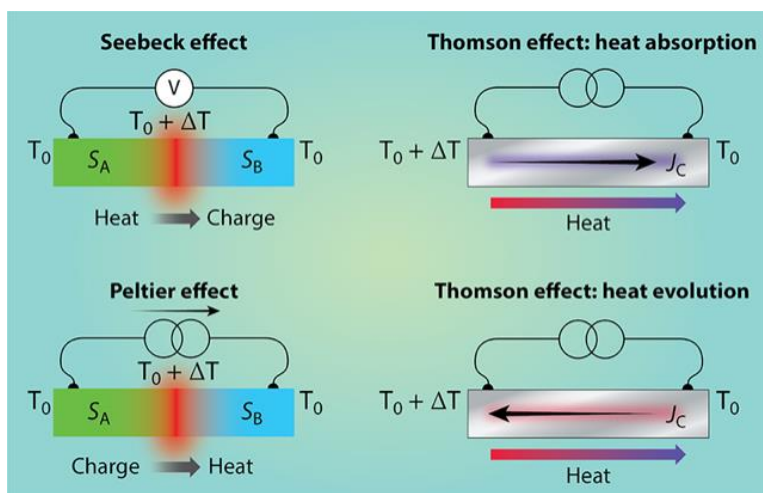


Figure 7. Thermoelectric effects (Morrison & Dejene, 2020)

## 2.4 Joule heating

Joule heating is the heat generated when an electric current passes through a conductive material. For the thermoelectric generator, the heat is generated in roughly equal proportions on the cold side as on the warm side. The electrical energy, in other words, the kinetic energy of the charge carriers in the case of ion conduction, is converted directly, in the case of electron or hole conduction, indirectly through scattering processes into undirected kinetic energy of the atoms and molecules of the conducting material (electrical conduction). This electrical energy converted into heat is also known as electrical heat equivalent. The amount of heat generated per unit of time and volume, that is to say, the thermal power density, is shown in the Equation below. (Spektrum.de, 2021)

$$\dot{q} = E * j = \rho j^2 \quad (5)$$

where,

$E$  = electric field strength

$j$  = current density

$\rho$  = specific resistance

This results in 1841 by J.P. Joule found Joule's law for the integral Joule heat in the conductor:

$$Q_{Joule} = U * I = R * I^2 \quad (6)$$

where,

$U$  = voltage

$I$  = current

$R$  = resistance

As can be seen from Equation (6), the current goes as square into the calculation and can therefore cause large losses with high current values. Therefore, in electrical circuits, a low electrical resistance and a low current flow are desired. Because of the different temperatures, the electrically conductive materials have different resistance. Therefore, different Joule heat is existing on the two sides of the TEG. In semiconductors, the resistance increases with decreasing temperature, the opposite behavior occurs when the temperature rises. This means that on the hot side of the TEG, a smaller Joule heat is generated than on the cold side. In practice, however, the variation in resistance should not be of great importance. However, it reduces in cooling applications the achievable lowest temperature of the cold side and increases the temperature of the hot side. Therefore, the additional generated heat must also be drawn off. (Schröter, 2008)

### 3 THERMOELECTRIC GENERATOR

Thermoelectric generators (TEG) are components that can convert temperature differences directly into electrical energy. A heat flow flows through the thermoelectric generator, and as a result of the temperature difference between the two sides, an electrical DC current is produced. A typical thermoelectric generator can, for example, with a heat flow of 100 watts generate 5 watts of electric power. The voltage can be up to 10 volts with a current strength of 0,5 A. The thermoelectric generator must be heated continuously on one hand and continuously cooled on the other to maintain electricity production. Unfortunately, only a fraction of the heat is converted into electricity. The greater the temperature difference at the thermoelectric generator, the greater the proportion of electricity generated and the higher the electrical efficiency. For every 30 °C temperature difference, approximately 1% of the heat flow is converted into electricity. If, for example, the temperature difference is 150 °C, about 5% of the heat is converted into electricity. (Qick-Ohm, 2021)

Much research must be done to improve the efficiency of TEGs. Ideally, there would be no heat conduction at all in the semiconductors, and a heat flow would only come about because the electrical charge carriers carry the current transport heat. In theory, TEGs are limited to the Carnot efficiency, which also applies to any heat engine. (RP-Energie-Lexikon, 2020)

#### 3.1 Carnot efficiency

Carnot efficiency is the maximum efficiency that a heat engine may have operating between the two temperatures (ScienceDirect, 2022). This maximum efficiency is set by the Second Law of Thermodynamics. The law was derived by Sadi Carnot in 1824. The Second Law of Thermodynamics describes the limitations of heat transfer. It sets out the specific idea that heat cannot be converted entirely to mechanical energy, as illustrated in Figure 8 below and in Equation (7). (Energy Education, 2022)

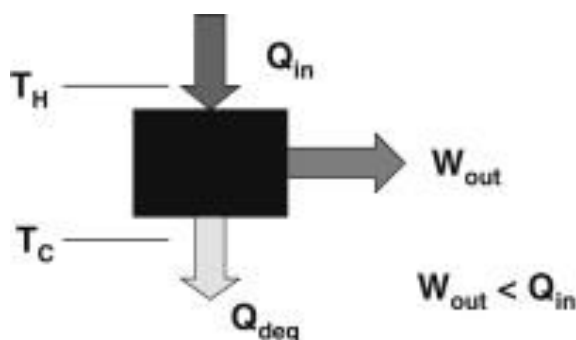


Figure 8. Principle of Carnot efficiency. (ScienceDirect, 2022)

$$\eta = \frac{W_{\text{out}}}{Q_{\text{in}}} = 1 - \frac{T_c}{T_h} \quad (7)$$

where,

$W_{\text{out}}$  = mechanical output work

$Q_{\text{in}}$  = input energy

$T_h$  = temperature of hot source

$T_c$  = temperature cold sink

The term  $Q_{\text{deg}}$  in Figure 8 is the waste heat of the heat engine. The lower this value is the higher is the Carnot efficiency, but it can never reach 100%.

### 3.2 Working principle of TEG

As already mentioned, thermoelectric generators are based on the Seebeck effect, such as the thermocouple. A thermocouple can only generate a maximum voltage of 0.1V. In a TEG many of these thermocouples are connected electrically in series and thermally in parallel. Figure 9 shows the structure of a TEG (a) together with the equivalent electrical circuit (b), where  $N$  is the number of connected thermocouples,  $\alpha_{AB}$  is the Seebeck coefficients of the two joined materials A and B forming the thermocouple ( $\alpha_{AB} = \alpha_A - \alpha_B$ ). (ScienceDirect, 2020)

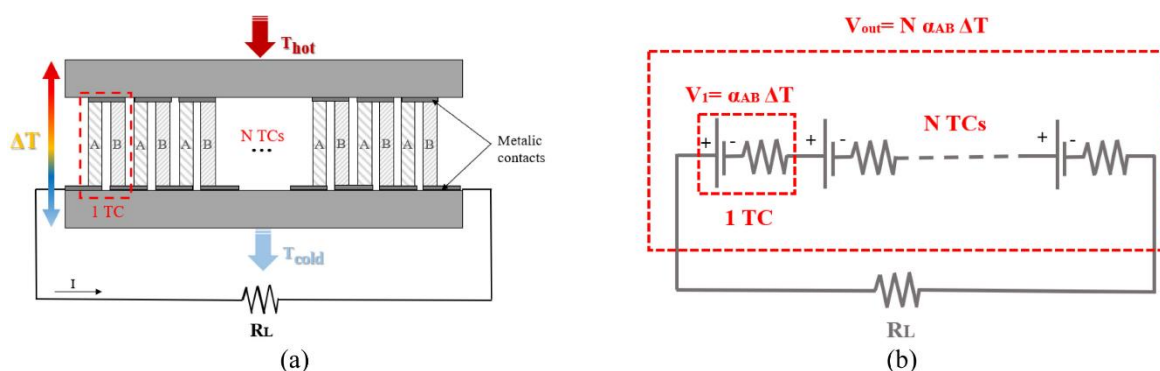


Figure 9. Typical TEG: (a) Basic principle, (b) Equivalent electrical circuit (ScienceDirect, 2020)

When the TCs are connected electrically in series, the total internal resistance is proportional to their number  $N$ . So, even though a high number of TCs will increase the voltage delivered by the TEGs, its impact on the internal resistance is adverse (Figure 9b). Indeed, the increase of series connected TCs number will lead to a rise of the TEG's internal resistance, which is expressed in the Equation (8). (ScienceDirect, 2020)

$$R_{TEG} = N \left( \frac{\rho_A L_A}{S_A} + \frac{\rho_B L_B}{S_B} + 2 \frac{\rho_C L_C}{S_C} \right) \quad (8)$$

where,

$\rho_A$  and  $\rho_B$  = electrical resistivity of material A and B

$\rho_C$  = electrical resistivity of the metallic contacts

$L_A$  and  $L_B$  = arm length of the thermocouples crossed by the heat flow

$L_C$  = contact length

$S_A, S_B, S_C$  = cross-sectional area of the thermocouples A and B and the contacts

The delivered output power of the generator is given by (ScienceDirect, 2020):

$$P = V_{out}^2 \frac{R_L}{(R_{TEG} + R_L)^2} \quad (9)$$

where,

$R_L$  = load resistance

$R_{TEG}$  = internal resistance

If the load resistance is matching the internal TEG's resistance,  $R_{TEG}$ , the maximum output power is expressed as (ScienceDirect, 2020):

$$P_{max} = \frac{V_{out}^2}{4R_{TEG}} \quad (10)$$

where,

$V_{out}^2$  = second Power of output voltage

$R_{TEG}$  = internal resistance

Applications for TEGs have been existing already for many years. First TEGs have been built already in the 19th century. In 1930 the Cardiff Gas Light & Coke gas-operated radio was introduced, where a gas-operated thermoelectric generator is used to power a radio. Another example is the energy supply of satellites, which cannot be realized with solar energy outside the solar system or at a great distance from the sun. Since 1977 spacecrafts like the "Voyager 1" or the Mars rover "Curiosity" (Figure 10) are powered by radioisotope thermoelectric generators, or RTGs. They provide electrical power by converting the heat generated by the decay of plutonium-238 (Pu-238) fuel into electricity using thermocouples. Since they have no moving parts that can fail or wear out, RTGs have historically been viewed as a highly reliable power source. Thermocouples have been used in RTGs for a total combined time of over 300 years, and not a single thermocouple has ever ceased producing power. (NASA, 2020).

TEGs have many more advantages such as relatively simple design, compact size, relatively easy scalable and they have ecological cleanliness and safety because of the lack of any gases and liq-

uids. They produce no noise or vibrations since there are no moving parts. The operation is independent from any orientation, even from gravity and zero gravity. The generation of electrical energy is directly from heat. Peltier elements can be used for cooling or heating simply by reversing the polarity of the direct current, which makes them ideal for precise temperature control. When using Peltier elements for heating they are more efficient as resistance heaters. This is because they can use the input power to generate heat plus the heat caused by the heat pump effect. Practically there are unlimited possibilities for their use, down to the smallest size. (Quick-Cool 1, 2021)



Figure 10. Self-portrait of NASA's Curiosity Mars rover (NASA, 2020)

### 3.3 Structure of the TEG

When talking about TEGs the actual device is a Peltier element which, as already mentioned, can be used for cooling or heating by applying a DC current, to it with the desired direction of the current flow. The term thermoelectric generator (TEG) is used when due to the temperature difference between the two sides of the Peltier element a current flow occurs. Since this paper is concerned with the production of electric energy the term TEG is mostly used. Figure 11 shows a thermoelectric generator module type TEC1-12706, which is used later in an experimental setup.

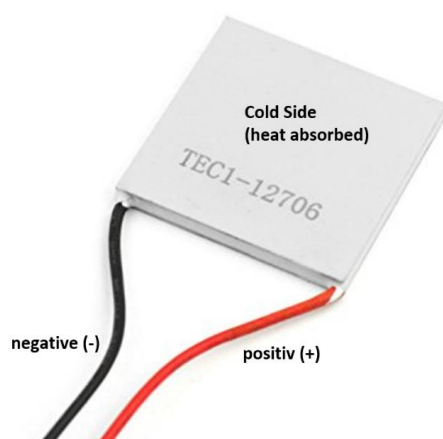


Figure 11. TEC Module type TEC1-12706. (Meerstetter Engineering, 2022)

TEGs are usually composed of p-type and n-type semiconductors because they have lower thermal conductivity than metal. The lower electrical conductivity compared to metal is compensated by the higher Seebeck coefficient as seen in Table 1. The most widely used material for Peltier elements is currently Bi<sub>2</sub>Te<sub>3</sub> (bismuth telluride). This starting material is made into a cuboid shape and soldered between electrically insulating surfaces. In most cases, this is aluminum oxide (Al<sub>2</sub>O<sub>3</sub>). (QUICK-OHM, 2021) Figure 12 shows the schematic of a commercial Peltier element which in turn can be used as a thermoelectric generator.

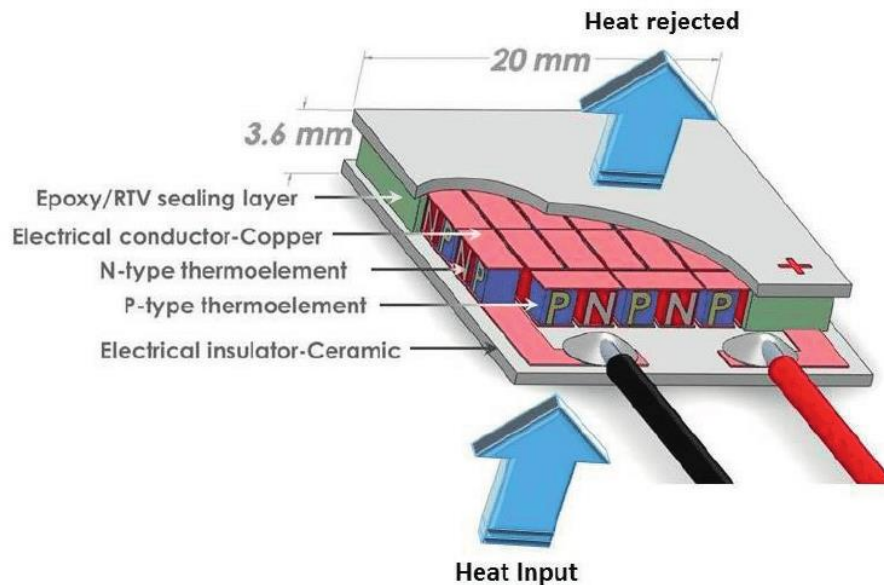


Figure 12. Schematic of a commercial thermoelectric generator module (Faraji, Date, Singh, & Akbarzadeh, 2014)

### 3.4 Semiconductor

The semiconductor material of one leg is p-, that of the other is n-doped (semiconductor P and semiconductor N in Figure 12). Because of this, the necessary different Seebeck coefficients are achieved, as it can be seen in Table 1. The difference for p- doped bismuth telluride and n-doped bismuth telluride is significant compared to other material combinations.

Depending on whether a positively or negatively conductive semiconductor material is needed, the doping procedure is different. For positive conductive semiconductors trivalent foreign atoms such as Boron (B), Aluminum (Al), Germanium (Ge), or Indium (In) are incorporated into tetravalent semiconductor materials, an increased charge carrier density in the valence band at  $T > 0$  K occurs. For example, in Figure 13 (left side) the incorporation of gallium creates a free positive hole. Such a defect is called *acceptor*. Another electron then occupies this hole and another occupies the newly created hole, etc. The hole moves in the opposite direction to the electrons, a current is flowing. This process is called p-doping; thus, one speaks of p-semiconductors.

For a negatively conductive semiconductor material Si (or Ge) is deliberately contaminated with pentavalent atoms such as P, As or Sb, an increased charge carrier density in the conduction band is observed at finite temperatures. On (right side) shown below, arsenic creates an additional electron. This is only weakly stationary and can be caused to wander by an increase in temperature or applied voltage. A current is flowing. This interference is called *donor*, the semiconductors doped in this way are called n-semiconductors.

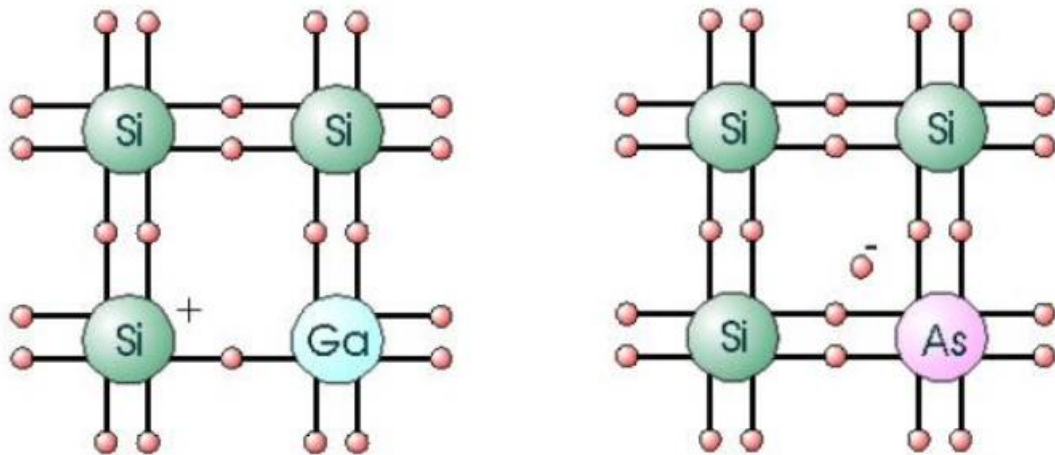


Figure 13. Schematic representation of p-doping (left) and n-doping (right). (Helmholtz-Zentrum Dresden-Rossendorf, 2010)

### 3.5 TEG design approaches

There are three design approaches of TEGs that differ according to the thermocouples' arrangement on the substrate regarding the heat flow direction, which are: (i) Lateral heat flow, lateral TCs arrangement; (ii) Vertical heat flow, vertical TCs arrangement; and (iii) Vertical heat flow, lateral TCs arrangement. (ScienceDirect, 2020)

The first TEG design uses a lateral TCs arrangement to convert a lateral heat flow,  $Q_h - Q_c$ . In this design, also called planar TEG, thermocouples are printed, patterned, or deposited on the substrate surface (Figure 14). The main advantage of this approach lies in its ability to manipulate the thickness and the length of each thermocouple arm combined to, its suitability with thin film deposition, which allows creating thinner and longer thermocouples compared to other types. Besides, this arrangement increases the thermal resistance of the thermoelements compared to other TEGs designs because of using lengthy TCs arms which leads to a temperature gradient increasing along this latter, and eventually, an output voltage rising. (ScienceDirect, 2020)

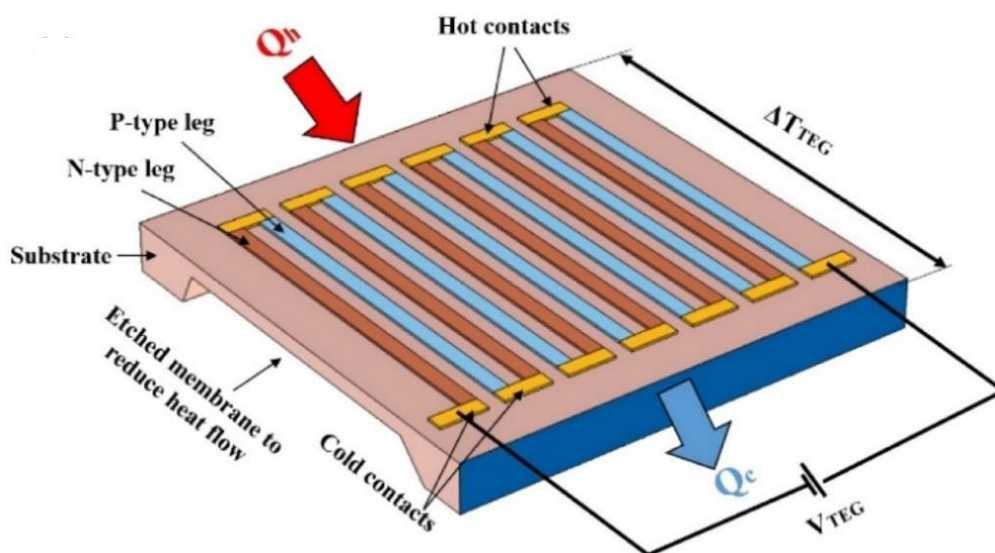


Figure 14. Planar TEG design. (ScienceDirect, 2020)

In the second TEG design, TCs arranged vertically between the heat source and the heat sink (Figure 15). Thus, the heat is flowing vertically along the thermoelement arms and the substrates. This arrangement is similar to the Peltier-based module for refrigeration. This kind of TEGs provides high integration density, and is the most commercialized because of its simplicity, high TCs integration, and high output voltage. (ScienceDirect, 2020)

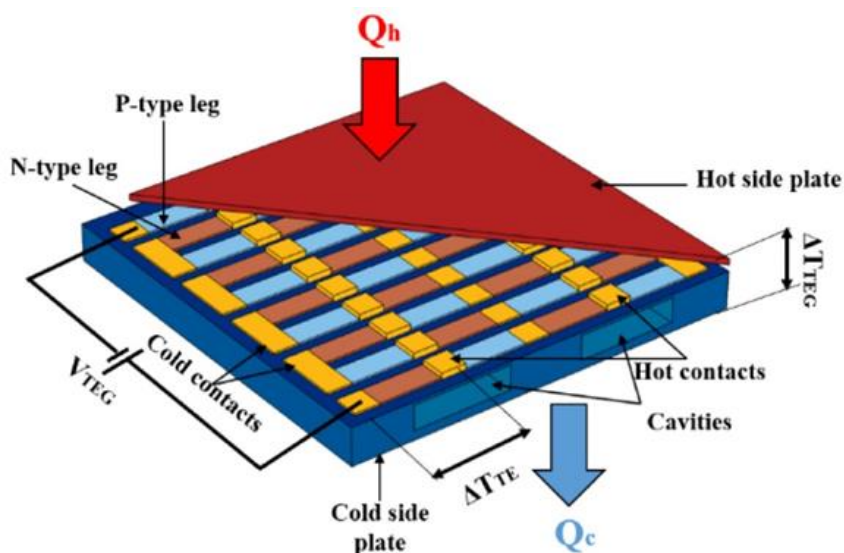


Figure 15. Vertical TEG design. (ScienceDirect, 2020)

The last TEG design, referred to as mixed, is made by TCs mounted laterally on the substrate, while the heat flows vertically (Figure 16). The vertical heat transfer was instigated through the integration of micro-cavities into the substrate, located under the thermocouple arms. (ScienceDirect, 2020)

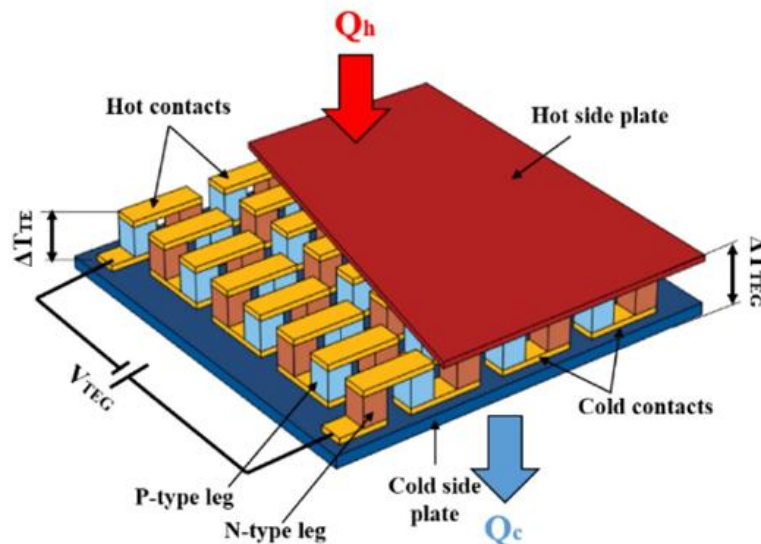


Figure 16. Mixed TEG design. (ScienceDirect, 2020)

Besides the structural approaches, there are also different physical design approaches. Thermoelectric generators can have a cascaded design, such as a double or triple layer. With this design can be achieved a higher temperature difference between the hot and cold side. Figure 17 shows an example of such cascaded or multistage thermoelectric element. There are also different physical shapes available, such as curved TEGs or with holes for easier mounting.



Figure 17. Multistage thermoelectric generator. (Laird Thermal Systems , 2020)

### 3.6 Output voltage and current

The output voltage of a TEG is determined, among other things, by its internal structure and the interconnection of the cascades. With different options it is basically possible to generate any required voltage level. The more thermocouples a TEG has, the higher the electrical voltage generated. The greater the electrical (ohmic) internal resistance of the TEG, the higher the voltage and the lower the strength of the generated current. (Qick-Ohm, 2021) The open circuit voltage of a pair of legs in the TEG is directly influenced by the temperature difference and the Seebeck coefficient as expressed in Equation (1). In operation, however, the open circuit voltage is not of great importance, as normally a load is connected. (Schröter, 2008)

The voltage at the load  $U_{load}$  [V] is calculated according to Ohm's law from the load resistance  $R_a$  [ $\Omega$ ] connected to the TEG and the load current  $I_{load}$  [A]. If the external resistance  $R_a$  is assumed to be constant and the load current  $I_{load}$  increases in the direction of the short-circuit current, the load voltage  $U_{load}$  decreases towards zero. When the load current  $I_{load}$  becomes zero, the Load voltage  $U_{load}$  reaches its maximum value, the open circuit voltage. (Schröter, 2008)

$$U_{load} = R_a * I_{load} \quad (11)$$

The applied load current  $I_{load}$  [A] in Equation (11) is calculated based on Equation (12) from the thermal voltage  $U_{th}$  [V], which is derived from Equation (1), the internal resistance  $R_i$  [ $\Omega$ ] and the connected load resistance  $R_a$  [ $\Omega$ ]. In operation, the load current  $I_{load}$  is therefore only dependent on the thermal voltage  $U_{th}$ , since the internal resistance of the TEG and the load resistance can be assumed constant. According to Ohm's law a higher thermal voltage results in a higher current flow. (Schröter, 2008)

$$I_{load} = \frac{U_{th}}{R_i + R_a} \text{ as} \quad (12)$$

The Equations (1), (11) and (12) can be combined, which lead to the Equation for the load voltage  $U_{load}$  [V]. To simplify matters, the Seebeck coefficients  $\alpha_1$  and  $\alpha_2$  [V / K] are replaced by the Seebeck coefficient  $\alpha$  specified by the manufacturer like in Table 1. Seebeck coefficient of materials. The temperatures  $T_h$  and  $T_c$  [K] are replaced by  $\Delta T$ .

$$U_{load} = R_a * \frac{\alpha * \Delta T}{R_i + R_a} \quad (13)$$

From this equation it can be seen that, if the resistances and Seebeck coefficients are considered constant, the load voltage depends directly on the temperature difference at the TEG, meaning a high temperature difference results in a higher load voltage.

### 3.7 Electrical Power

The performance of a TEG, such as used later in the experimental setup is in the range from 0,5 to around 1 Watt per module. The dimensions are between 40 mm x 40 mm. If greater performance is required, the modules can be divided into connected in parallel or in series. The electrical power  $P_{el}$  [W] is calculated according to Equation (14).

$$P_{el} = U_{load} * I_{load} \quad (14)$$

combining Equation (12) and (13) results as well the electrical power  $P_{el}$  [W]:

$$P_{el} = R_a * \left( \frac{\alpha * \Delta T}{R_i + R_a} \right)^2 \quad (15)$$

The regulation of the performance of TEG, as be seen from emerged Equation (15), can only be achieved by varying the load resistance  $R_a$  [ $\Omega$ ] or the temperature difference  $\Delta T$  [K] respectively. This principle must be considered for the design of a TEG system.

### 3.8 Heat supply, heat removal and heat development

Three different types of heat occur at the TEG: Joule heat  $Q_{Joule}$  [W] from Equation (6), the Peltier heat  $Q_{Peltier}$  [W] from Equation (16):

$$Q_{Peltier} = \alpha * T * I_{load} \quad (16)$$

and the heat conduction  $Q_{wl}$  [W] from Equation (17):

$$Q_{wl} = \beta_{wl} * \Delta T \quad (17)$$

where,

$Q_{wl}$  = heat conduction [W]

$\beta_{wl}$  = thermal conductivity [W / K]

$\Delta T$  = temperature difference [K]

The Joule heat has little influence on the efficiency because it not only warms the cold side, but also the hot side. Therefore, on the hot side, less heat must be absorbed, as can be seen from Equation (18). This gain, however, becomes a loss on the cold side and is canceled out. However, the additional heat on the cold side must be dissipated, which leads to a greater technical effort. The temperature difference on TEG itself remains unaffected. (Schröter, 2008)

The Peltier effect from Equation (16) has a negative influence on the efficiency. This heat has to be supplied and also removed again. Because of this effect there is a heat flow from the hot to the cold side of the TEG. This heat flow depends directly on the temperature  $T$  [K] and the load current  $I_{load}$  [A]. With linear temperature rise, the load current also rises linearly, which leads to a heat flow with square magnitude. (Schröter, 2008)

The third heat is the heat flow through direct heat conduction in the material. The heat conduction is shown in Equation (17) and behaves linearly. The thermal conductivity  $\beta_{wl}$  [W / K] of the TEG can be assumed to be constant and thus only the temperature difference  $\Delta T$  [K] has an effect. (Schröter, 2008)

All these heat flows occurring at the TEG are undesirable. When the heat flow flows from the hot to the cold side, the result is an equalization of the hot and cold temperatures. The thermoelectric voltage is generated by maintaining the temperature difference as stated in Equation (1). If there is not enough heat supplied or the supplied heat cannot be dissipated a temperature equalization takes place, which is to avoid. To achieve a high efficiency of the TEG a high thermal resistance in the Seebeck leg pair is needed, to keep the heat flow as low as possible. Low thermal resistance on the outside of the TEG ensures that the temperature difference is applied directly to the pair of Seebeck legs and thus the thermal voltage is high. Figure 18 below shows the types of heat applied at the TEG with their direction of flow. (Schröter, 2008)

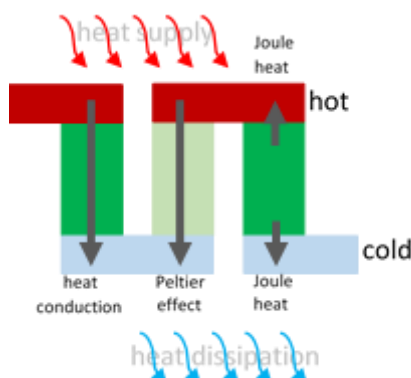


Figure 18. Types of heat at a TEG.

To determine the supplied heat  $Q_{in}$  [W], Equation (6) for the Joule heat, Equation (16) for the Peltier effect with  $T_{hot}$  [K] and Equation (17) for heat conduction are combined into Equation (18). Only half of the Joule heat will be included in the calculation because it is applied on both sides of the TEG. The other two effects do not occur on the outer sides of the TEG. They represent a heat transport through the TEG. The total term is negative because it is a question of heat absorption. (Schröter, 2008)

$$Q_{in} = \frac{Q_{Joule}}{2} - Q_{Peltier} - Q_{wl} \quad (18)$$

Summarized and simplified, the following Equation presents the supplied heat  $Q_{in}$  [W] for the TEG:

$$Q_{in} = \frac{1}{2} * R_i * \left( \frac{\alpha * \Delta T}{R_i + R_a} \right)^2 - \frac{\alpha^2 * T_{hot} * \Delta T}{R_i + R_a} - \beta_{wl} * \Delta T \quad (19)$$

To determine the heat dissipated by the TEG, all terms from the Equation (18) are added together, which gives the and give the heat emission  $Q_{out}$  [W]. It should be noted that in Equation (16) for the Peltier heat  $T_{cold}$  [K] must be used, since it is on the heat-dissipating side. This term becomes positive because heat is emitted.

$$Q_{out} = \frac{Q_{Joule}}{2} + Q_{Peltier} + Q_{wl} \quad (20)$$

The summarized and simplified Equation for the needed heat dissipation  $Q_{out}$  [W] at the TEG is as follow:

$$Q_{out} = \frac{1}{2} * R_i * \left( \frac{\alpha * \Delta T}{R_i + R_a} \right)^2 + \frac{\alpha^2 * T_{cold} * \Delta T}{R_i + R_a} + \beta_{wl} * \Delta T \quad (21)$$

### 3.9 Cooling off thermoelectric generators

The cooling of the thermoelectric generator is an important factor for good performance and high efficiency. If the heat is not sufficiently discharged, it comes to heat accumulation in the system. The result is a reduction of temperature gradient and decrease in electrical power and the efficiency of the TEG. There are several ways to remove the heat from the TEG in order to maintain the needed difference in temperature between the hot and cold side of the Peltier element.

#### 3.9.1 Natural convectional cooling

With natural cooling, the heat loss is dissipated by natural drafts (air self-cooling). The heat sink gives off heat to the environment through natural (free) convection and radiation. Convection and radiation are temperature dependent. Therefore, the thermal resistance of a heat sink decreases with air self-cooling as the power dissipation increases. The inflow and outflow of the cooling air must be as unhindered as possible. The heat sinks should be preferably mounted vertical to make use of the chimney effect. The chimney effect is the tendency of air or gas in a shaft or other vertical passage to rise when heated, owing to its lower density compared with that of the surrounding air or gas. Finned heat sinks for example make use of natural convection.

#### 3.9.2 Forced convectional cooling

The forced convectional cooling increases the convectional cooling effect by adding a fan, which increases the airflow. Also, the direction of the cold airflow can be forced into the needed direction. This is the case, for example in PC power supplies. Here the direction of airflow is horizontal. For TEG applications the downside is the need for additional electrical energy which uses up electrical energy produced by the TEG and thus reduces the output performance.

#### 3.9.3 Liquid cooling

The cooling of thermoelectric generators with liquid is the most effective way. Here the heat is transferred through conduction. The liquid can transport much more thermal energy away from the TEG than air. In this system again is additional electrical energy needed for the pump, which keeps the liquid moving inside the cooling system.

### 3.10 Efficiency

The current efficiencies of TEG are not very high. By a temperature difference of 100 K, depending on the module, it is around 4 to 5 % (See Figure 19). Bigger efficiencies can be achieved with larger temperature differences, as seen from Figure 20. Here is to mention that the limit for simple TEG-modules lies around 250 °C at the hot side, since at higher temperatures the solder connection of the semiconductor and copper parts begin to loosen. Temperatures towards cold below normal ambient temperature mean additional energy expenditure for cooling. Therefore, the possible temperature range and thus the efficiency is limited from this side. Special developments for the high temperature range are excluded. The efficiency of TEG is calculated according to Equation (22), resulting from Equation (15) and Equation (18).

$$\eta = \frac{P_{el}}{Q_{in}} * 100 \quad (22)$$

As already explained, the influencing variables on the TEG are the Seebeck coefficient  $\alpha$ , the thermal conductivity  $\beta_{wl}$  [W/K], the resistances  $R_i$  and  $R_a$  [ $\Omega$ ] as well as  $\Delta T$  [K]. At the TEG itself, only  $\Delta T$  and  $R_a$  can be influenced for the regulation since the other values are fixed by the material. The ideal case in terms of efficiency always results from adjusting resistances  $R_i$  and  $R_a$ . Meaning that the load resistance must correspond to the internal resistance of the TEG, hence  $R_i = R_a$ . (Schröter, 2008)

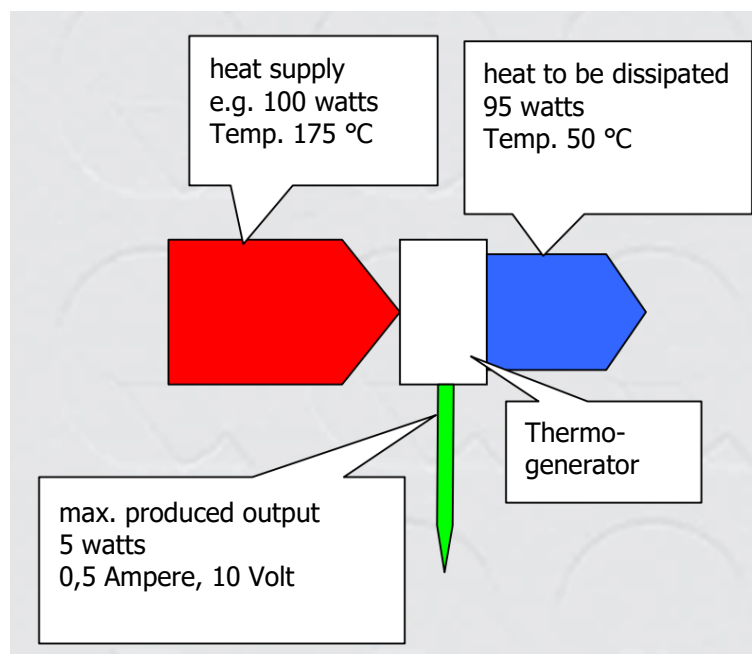


Figure 19. Thermoelectric generator output. (quickcool-shop, 2021)

When the load resistance is reduced, the current flow in the TEG increases conditionally by Ohm's law. This has the consequence that the heat flow, caused by the Peltier effect and the Joule heat, increases by leaps and bounds. This also increases the heat absorbed and removed again. The electrical power drops slightly because the voltage at the TEG drops sharply, due to the high Current

flow, which also applies to the efficiency. Only the heat conduction through the TEG remains constant, as this only depends on the material constants and the temperature gradient. (Schröter, 2008)

If the load resistance is increased, the current flow in the TEG decreases, with the result that the heat flow due to the Peltier effect and the Joule heat drops very sharply. This reduces the absorbed and removed heat. The electrical power rises to a higher level as the voltage on the TEG passes through, the lower current flow goes in the direction of the no-load voltage.

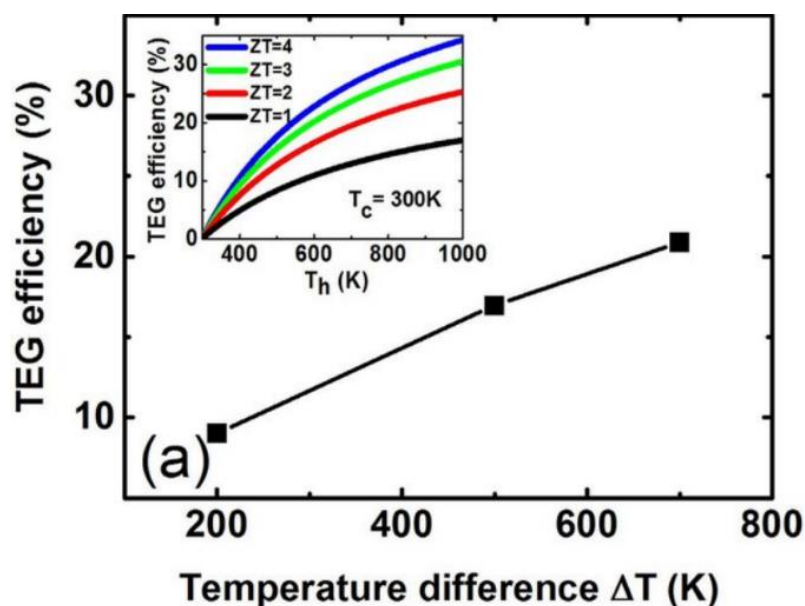


Figure 20. TEG Efficiency vs. temperature differences. (Ouyang, 2016)

### 3.10.1 Efficiency calculation

To get an idea of the economic efficiency, here is a rough example calculation with the following conditions. The thermoelectric generator is mounted directly to the heat source. The temperature of the hot side of the thermoelectric generator is 130 °C and the cold side is 50 °C. The thermoelectric generator must be connected to a heat sink with considerable effort (for each kWh of electricity generated, approx. 30 kWh of heat must be "moved"). The electricity generated can be fed to the grid or to the building's own network. Using a high-quality product (30 € for a 5 watts element; 5 watts<sub>eff</sub>) leads to approximately 14000 €/kW. (quickcool-shop, 2021)

Since the kiln is a periodic kiln, the annual usage of 7500 hours per year and a service life of 10 years can be assumed. This results in electricity production costs of approx. 19 cents/kWh (excluding maintenance, repairs, insurance, interest on capital, overheads).

This price is only marketable when there is no other option to generate electricity. This may apply to remote objects, in the case of military use or when there is a need to have an uninterrupted auxiliary power supply. This raises the question of what a power supply may cost if an alternative is missing. (In the desert, a glass of water is sometimes of immense value). (Quick-Cool 2, 2022)

However, the sensitivity of this price to the various influencing parameters must be repeatedly emphasized. For example, with a temperature gradient of approx. 50 °C and a usage time of approx. 1,000 h, with the mentioned influencing parameters, the electricity price is 180 cents/kWh!

### 3.11 TEG operating conditions

There are many conditions for the use of the thermoelectric generators, such as the environment of installation, whether it is installed on a fixed place such as an exhaust stack or in a moving place like in a car next to the exhaust pipe or inside the cooling system of the motor. The operational temperature is also an important aspect to consider.

#### 3.11.1 Temperatures

The most important condition for TEGs in applications is the temperature. On the one hand, the temperature should not destroy the TEG module, on the other hand, the temperature difference should be as high as possible to achieve high efficiencies and voltages. Common TEGs offer maximum operating temperatures between 100 and 250 °C. The reason for this is the limited melting temperature of the used solder joining the semiconductor and the copper bridges. There are also high temperature TEG models with operating temperatures of up to 1000 °C, which are mostly used for measurement purposes.

#### 3.11.2 Vibrations

Mechanical vibrations applied to a TEG can cause material fatigue and thus damage or destruction of the TEG module. An elastic thermal adhesive, as shown in Figure 21, can act as a vibration absorber between the heat exchangers and the TEG module. Ideally, no vibrations are applied to the TEG module. To find out the vibration resistance and the associated life span a bench test with different concept variations must be performed.



Figure 21. Attenuation with elastic thermal adhesive.

#### 3.11.3 Corrosion

Corrosion is another important criterion. The TEG should be designed to work for the whole lifespan of a kiln without the need for replacement. When used in exhaust system high temperatures and harsh environmental conditions occur. Here are temperatures more than 300 °C. The most suitable place for mounting a thermoelectric generator to the exhaust system is outside the exhaust stack. Here, high temperature differences can occur in wintertime up to -40 °C and in summertime up to +

50 °C, depending on the climatic zone. These temperature fluctuations, increased humidity and rain-water cause corrosion directly in the TEG, between the TEG and exhaust stack as well as between the TEG and heat exchanger.

The aim should be the use of corrosion-free materials for the connection of the TEG. The inside of the TEG must be sealed to prevent corrosion. Otherwise, the materials used like copper, tin and lead as well as the semiconductor elements getting damaged in a short period of time and function failure would be the result. One possibility is the sealing of the module with silicone, epoxy resin or protective varnish. Alternatively, the entire system can be encapsulated from the environment. (Schröter, 2008) (Wärmemanagement, 2021) As for the heat exchanger, they are usually made of copper or aluminum while the latter is the cheaper and more widely used material. However, suitable processing, such as anodizing, should be applied to make the aluminum more corrosion resistant to ensure sufficient durability against environmental influences.

#### 3.11.4 Fastening of the TEG

The attachment of the TEG to the heat exchanger is next to the temperature the most important fact for the efficiency. An inadequate connection has poor heat conduction consequently, which in turn causes a sharp decline in performance of the element. Critical is, that between the hot side and the cold of the TEG a temperature difference of 100 K or more exists. The different thermal expansion has on the TEG module a bimetal effect. The module bulges and loosens the necessary contact for heat conduction over its whole area. An oppression of this reaction by clamping can cause mechanical damage to the TEG, as the cascade-shaped semiconductor legs inside the TEG element deform caused by the high mechanical stresses and thus can be damaged through material fatigue. Recommended clamping forces vary depending on TEG element between 1,25 – 1,50 N/mm<sup>2</sup>. It is essential for secure clamping to follow manufacturer's instructions. When combining several TEG modules to a generator group the deviations in the contacting surfaces of the heat exchangers and TEG elements to one another also play a crucial role. Recommended are height differences of max. 0,05 mm and parallelism deviations of max. 0,02 mm to achieve a good heat transfer. Larger deviations will result in deterioration of performance. These deviations can occur on the TEG as well as on the connecting surfaces and can be compensated with the help of thermal paste or adhesive. The thermal paste has a thickness of 0,03 mm a thermal conductivity of about 20 - 35 W/K. With a thicker layer this value decreases to the actual value of the thermal paste of up to 9 W/K. This behavior is because with a thin layer of thermal paste the uneven contacting surfaces are partially in direct contact with each other. Therefore, direct heat conduction is occurring, which on average is greater than the thermal conductivity of the thermal paste alone. It follows that the gaps and the layer thicknesses of the thermal paste must be as small as possible to achieve a minimum of thermal resistance. (Schröter, 2008)

#### 3.11.5 Lifespan

The service life of thermoelectric generators is very much dependent on the conditions of where they are used. Mechanical stresses, vibrations and temperatures above the application limits are

particularly detrimental to the life of the TEGs. Another leading variable is the number of temperature cycles. At permanent use with constant or only slightly fluctuating temperatures within the application limit and low voltages, the lifespan of thermoelectric generators is very long. (Schröter, 2008)

### 3.12 Future of TEG

In the field of TEG, there are ongoing developments through which a significantly increased efficiency of the modules can be demonstrated. The Fraunhofer Institute for physical metrology is currently a leader in this field and speaks of efficiencies around 30%. These higher efficiencies can only be achieved, according to Equation (4), with a higher Seebeck coefficient, lower heat conduction and higher temperature differences due to better temperature resistance of the TEG. Therefore, the efficiency data must also be considered in relation to the operating temperature. Due to higher temperatures, current TEGs also achieve higher efficiencies. If these efficiency improvements due to material developments are correspondingly large, together with the simple design, low production costs and maintenance-free, TEGs become interesting for all applications in the use of waste heat. This trend will lead to the further development of these systems in industry and is likely to be even stronger in the future. As an example, there have been promising achievements in research with new materials like purified polycrystalline tin selenide (SnSe), which is not only cheaper than bismuth-telluride ( $\text{Bi}_2\text{Te}_3$ ) but also more environmentally friendly. It has been reported that hole doped SnSe polycrystalline samples with reagents carefully purified and tin oxides removed exhibit a figure of merit (ZT) of roughly 3,1 at 783 K (Zhou, C., Lee, Y.K., Yu, Y. et al., 2021). Whereas TEGs today have a figure of merit (ZT) of 1,25.

## 4 EXPERIMENTAL SETUP

Besides the theoretical calculation for a potential thermoelectric generator system, which can be used at an industrial kiln, an experimental setup was built to see the actual performance of thermoelectric generators on a small scale. For the simulation a tiny exhaust stack was built like shown in Figure 22. The chosen dimensions are 120 mm x 120 mm in width, with a material thickness of 4 mm. This is due to the fact that a normal square steel tube based on European Standard EN 10219 (Cold formed welded structural hollow sections of non-alloy and fine grain steel) has these dimensions. The height is 600 mm. The exhaust stack is elevated 300 mm, so that a heat source can be easily placed under the exhaust stack. In the experiment Peltier elements of type TEC1 12706 are used, as shown in Figure 11. This Peltier element has a dimension of 40 mm x 40 mm and is sealed with silicone. It has a thickness of about 3,8 mm. It consists of 127 thermocouples. The maximum DC current going through the Peltier element is 6 A. The maximum operating temperature is 85 °C and the maximum temperature difference  $\Delta T = 70$  °C. The datasheet of this Peltier element is shown in Appendix 1. The choice of this Peltier element was simply because of the significantly low price. The same applies to the heat sink, which has the same dimensions of 40 mm x 40 mm with a height of 20 mm. The material is aluminum. Figure 24 shows a picture of the heat sink. Unfortunately, there was no datasheet available.

The original idea was to have the Peltier elements together with the heat sink arranged in different orders to see if this might influence the performance of the Peltier elements due to different convective cooling possibilities. One side of the Exhaust stack the Peltier elements were arranged in 3 columns and 4 rows (left side of Figure 22). The other two sides of the exhaust stack are arranged in 2 columns and 7 rows (right side of Figure 22). In total 40 Peltier elements are placed.

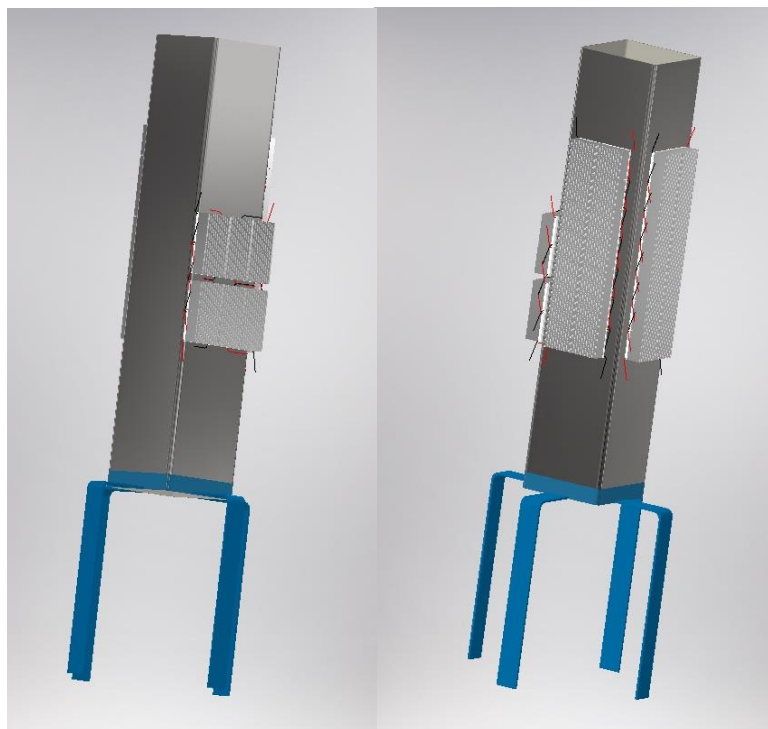


Figure 22. Design model of the Exhaust stack.

Before explaining the experiment further, it is necessary to mention that the outcome of this experiment was not as predicted. The electrical output energy was not nearly as theoretically calculated. The problem was realized but could not have been solved without having a completely new design of the experimental setup. The reason will be explained later. Still, it was good to do this experiment, because through this the difficulties of designing a thermoelectric generator system were realized. The experimental setup can be seen in Figure 23. It shows the exhaust stack with the mounted Peltier elements and heat exchangers. The electrical interconnection of the Peltier elements is concealed inside the conduits to hold the terminals, and to have not a too complicated look.

Below the exhaust stack is the heat gun, next to it is the DC / DC converter and a standard 12 VDC battery.



Figure 23. Experimental Setup.

## 4.1 Mounting

Before the Peltier element can be mounted it has to be determined which side of the Peltier element is the hot side facing the surface of the exhaust stack and respectively the cold side, bounded to the heat sink. A wrong sided installation of the Peltier element results in disfunction. For the chosen Peltier elements, the printed side is the cold side like shown in Figure 11.

Since the Peltier elements and the heat sinks are light weighted the mounting on the exhaust stack was done with thermal glue (see Figure 25) rather than clamping. This has the advantage of considerable easy mounting, and the thermal glue is working at the same time as thermal paste to smoothen the surface of the exhaust stack and give a good thermal conductivity as described in chapter 3.11.4. The downside of gluing the Peltier elements to the exhaust stack is that later changes in the outline are impossible, which during the experiment turned out to be a problem.

The thermal adhesive has high strength with good heat dissipation ( $W / m \cdot K$  1.7), and it can be easily applied and distributed because of its silicone-like consistency. The operating temperature is between  $-60\text{ }^{\circ}\text{C}$  and  $200\text{ }^{\circ}\text{C}$ . Drying time is approx. 20 min, hardening in approx. 24 hours, best results after approximately 150 operating hours. The manufacturer is AGIA TEX Germany, the EAN-number is: 4260632614334. (Kaufland, 2021)



Figure 24. Heat sink. (ebay, 2022)



Figure 25. AGIA TEX thermal adhesive. (Kaufland, 2021)

The Peltier elements are glued around the exhaust stack together with the heat sinks. The heat sinks are aligned so that the cooling fins are vertical oriented. In this way it is possible to make use of the uplift stream of the surrounding air of the exhaust stack because of the stack effect and thus get a possible good natural convection.

### 4.1.1 Stack effect

Stack effect, also called chimney effect, is a naturally induced vertical flow of air through a structure. It is caused by thermal differences. Higher-temperature air is less dense than cooler air. As the warmer air rises, it creates a pressure difference, with lower pressure below and higher pressure

above. For example, in a chimney the net effect is that warm air escapes from the top of the chimney, while cold air is drawn in at the bottom of the chimney (the fireplace), creating a self-sustaining upward flow of air (CPP Wind Engineering Consultants, 2022). The Same effect applies also to tall buildings where a possible powerful airflow must be considered. Good building design is making use of this effect, creating a natural air circulation in the building, thus reducing the need for air-conditioning systems and with this reducing energy costs. Figure 26 depicts the stack effect.

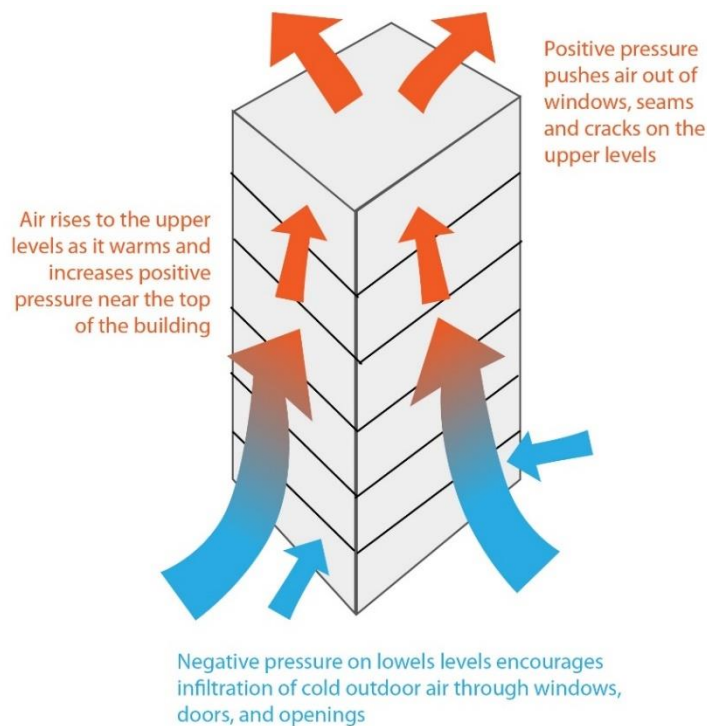


Figure 26. Principle of the stack effect. (AMI Environmental, 2022)

#### 4.2 Heat source

To simulate the heat coming from the kiln into the exhaust stack in a possible real situation a conventional heat gun with adjustable temperature level, as can be seen in Figure 23, was used. The output temperature can be adjusted between 50 °C and 600 °C. The temperature was at first set to 100 °C in order not to overheat the Peltier elements. After a while the temperature increased to the maximum temperature while monitoring the surface temperature of the exhaust stack model. At final state the temperature at the surface of the exhaust stack was measured with 50 °C. The temperature measurements at the experimental exhaust stack were obtained with the help of AstroAI True RMS 6000 Digital Multimeter capable of measuring temperatures. The experimental setup was done inside a building with a temperature of around 20 °C.

### 4.3 Electrical connection

Before the Peltier elements were connected to each other electrically, the proper function of the Peltier elements needed to be checked by measuring the internal resistance. Because during the measurement the resistance is rising due to the induced measuring current, the measured time was set to 30 seconds and then the obtained result was taken. As it turned out there were two Peltier elements with abnormal values, marked red in Table 3. One Peltier element had only a resistance of  $0,2 \Omega$  and can be assumed to have an internal short circuit. The other Peltier element had a resistance of  $15 \text{ k}\Omega$  and can be assumed to have an internal disconnection. Both cannot be used. Looking at the values of Table 3 it can be seen that some of the internal resistance values differ more than the others. This can be due to the fact of quality issues in the manufacturing process or actual different values as stated in the data sheet. The Peltier elements were not purchased from one supplier, because of delivery problems.

Table 3. Measured internal resistance of Peltier elements.

side one			side two		side three	
2,5 $\Omega$	2,2 $\Omega$	0,2 $\Omega$	15 $\text{k}\Omega$	2,8 $\Omega$	2,7 $\Omega$	2,4 $\Omega$
2,6 $\Omega$	2,1 $\Omega$	1,8 $\Omega$	2,9 $\Omega$	1,6 $\Omega$	2,5 $\Omega$	2,3 $\Omega$
			3,4 $\Omega$	1,7 $\Omega$	2,3 $\Omega$	2,2 $\Omega$
2,6 $\Omega$	2,6 $\Omega$	2,0 $\Omega$	3,2 $\Omega$	1,9 $\Omega$	2,4 $\Omega$	2,2 $\Omega$
2,5 $\Omega$	2,4 $\Omega$	1,7 $\Omega$	3,1 $\Omega$	2,6 $\Omega$	2,3 $\Omega$	2,2 $\Omega$
			2,6 $\Omega$	2,9 $\Omega$	2,5 $\Omega$	2,7 $\Omega$
			2,6 $\Omega$	2,9 $\Omega$	2,1 $\Omega$	2,0 $\Omega$

The electrical configuration of the TEG requires in terms of the temperature dependent output voltage, some effort. On the one hand should the system voltage be as high as possible to minimize losses due to low current. On the other hand, should the voltage be close to the electrical system where the voltage produced by the TEG is fed in. The best choice to meet these requirements is to use DC-DC converters. These regulate a variable DC input voltage to a fixed DC output voltage. DC-DC converters have a specific input voltage range. Therefore, the interconnection of the TEGs must be done in such way to comply with the corresponding input voltage range of the DC-DC converter.

When interconnecting voltage sources, it is essential to ensure that they are always assembled in the same circuits so that all partial circuits have the same output voltage. If this is not the case, the different voltages and resistances lead to current flows of the TEG under each other. As a result, the TEG partial circuits would work with lower output voltages and resistors, which is undesirable.

To make the connection as simple as possible the Peltier elements were electrically connected in three groups each having 12 Peltier elements connected in series. This meant to leave out, besides the two defective Peltier elements, two more out from the electrical connection. The chosen DC-DC converter (Appendix 2) is capable of accepting an input voltage of 6 – 36 VDC, which can be converted to an output voltage between 1,25 – 32 VDC. The output current can be adjusted between 0,05 – 5 A. These parameters appeared to be suitable for the experimental setup.

Additionally, the DC-DC converter can also be used as a battery charger. With this came the idea to connect the output to a 12 VDC Battery since it would simulate as best a potential real thermoelectric generator used at a kiln exhaust stack. Connecting the thermoelectric generator to a Battery would as best deal with the fluctuation in electrical output of the thermoelectric generator since the kiln is not continuously working, nor at constant temperature and therefore the temperature of the exhaust stack will be not constant. Figure 27 show the electrical connection together with DC / DC converter and the load. The three in groups are highlighted in different colors, where group 1 (green) of serial connected Peltier elements has a total resistance of  $27,6 \Omega$ , group 2 (yellow) has a total resistance of  $31,6 \Omega$  and for group 3 (orange) the total resistance is  $27,7 \Omega$ . The resistance of all three groups combined in parallel is  $9,6 \Omega$ .

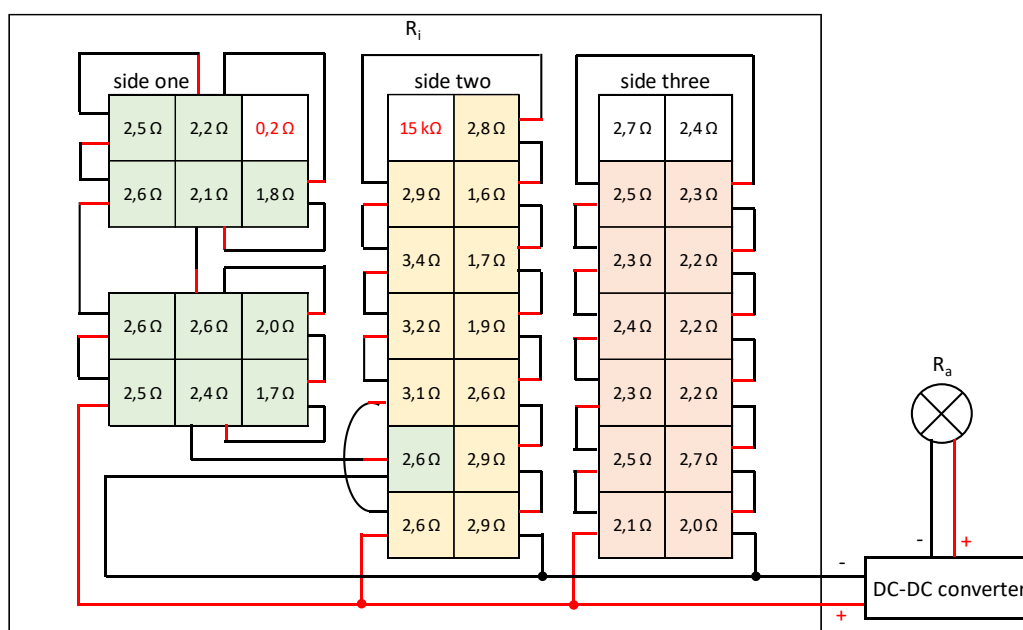


Figure 27. TEG electrical connection.

#### 4.4 Theoretical electrical output power

The theoretical output power of the TEG can be determined before the actual electrical connection is made. Unfortunately, from the datasheet for the Peltier element in Appendix 1, cannot be seen the possible produced voltage based on the Seebeck effect. The used Peltier elements are made of doped Bismuth telluride. Based on the entries in Table 1 this material pair generates a voltage  $U_{th}$  of around  $200 \mu\text{V}$  per Kelvin temperature difference. Having 127 pairs and an assumed temperature difference  $\Delta T$  of 30 K the open circuit voltage can be calculated based on Equation (1).

$$U_0 = U_{th} * N * \Delta T = 0,0002 \frac{\text{V}}{\text{K}} * 127 * 30 \text{ K} = 0,76 \text{ V} \quad (23)$$

The internal resistance of the Peltier element at temperature  $T= 50\text{ }^{\circ}\text{C}$  is, according to the datasheet in Appendix 1, around  $2,2\ \Omega$ . This leads to a short circuit current, based on the Equation below, of  $0,75\ \text{A}$ .

$$I_c = \frac{U_0}{R_i} = \frac{0,76\ \text{V}}{2,2\ \Omega} = 0,35\ \text{A} \quad (24)$$

As described in chapter 3.10, to achieve the maximum amount of electrical power from a voltage source the load resistance  $R_a$  should match the internal resistance  $R_i$ , hence  $2,2\ \Omega$ . The current that then arises is, based on Equation (12), calculated as follows:

$$I_{\text{load}} = \frac{0,76\ \text{V}}{2,2\ \Omega + 2,2\ \Omega} = 0,17\ \text{A} \quad (25)$$

The maximum power results from Equation (14)

$$P_{el} = U_{\text{load}} * I_{\text{load}} = 0,76\ \text{V} * 0,17\ \text{A} = 0,13\ \text{W} \quad (26)$$

In summary, one Peltier element TEC1 12706 with an internal resistance  $R_i= 2,2\ \Omega$  can generate an output power of  $0,13\ \text{W}$  if the temperature at the hot side is  $50\text{ }^{\circ}\text{C}$  and at the cold side  $20\text{ }^{\circ}\text{C}$ . In Chapter 3 it was described that for every  $30\text{ }^{\circ}\text{C}$  temperature difference, approximately 1% of the heat flow is converted into electricity. To actually get the  $0,13\ \text{W}$  electrical power from one Peltier element an input heat flow of  $13\ \text{W}$  is needed.

Adding the 12 Peltier elements for each group together, assuming the internal resistance of all Peltier elements is equal to  $2,2\ \Omega$ , the output voltage is  $9,1\ \text{V}$  and the output power rises to  $1,58\ \text{W}$ . The combination of all Peltier elements gives an output power of  $4,75\ \text{W}$ . Just enough to lighten up a bicycle lamp. These numbers are unfortunately not very high. This is due to the small difference in temperature.

#### 4.5 Conclusion of the experimental setup

As already mentioned in Chapter 4 the outcome of the experiment was not successful. While the air inside the exhaust stack was heated by the heat gun as described in Chapter 4.2 the output voltage of the thermoelectric generated was monitored with a Multimeter. With the rising temperature, the output voltage was rising as well. The maximum reached output voltage of the TEG was  $5,66\ \text{V}$ . In addition to measured value of the multimeter the display of the DC / DC converter was also observed. As seen in Figure 28 both values are similar. The  $5,66\ \text{V}$  output voltage was just enough to get the DC / DC converter in running mode, but not enough to charge the battery. Therefore, a normal  $6\ \text{VDC}$ ,  $5\ \text{W}$  lamp was connected to a visual verification of the function of the thermoelectric generator.

The measured temperature of 50 °C at the hot side of the Peltier element was taken at the outer surface of the exhaust stack next to a Peltier element. The cold side was measured at the surface of the heat sink. The measured value was 46 °C. These results show the main problem of the failed experiment. The heat sink could not dissipate enough heat to the ambient air to maintain a suitable temperature difference. Another problem was that the resistance to the three groups of Peltier elements is not exactly the same. A low thermal conductance due to improper mounting can be ruled out since the temperature difference between the hot and cold side of the Peltier element is small. Further testing could be done, especially in the design of the electrical interconnection to find a better solution. The performance of the TEG could be increased by increasing the air flow going through the heat sinks. Placing a small fan under the heat sinks could increase the heat dissipation of the heat sink and thus get a bigger temperature difference across the TEG module.

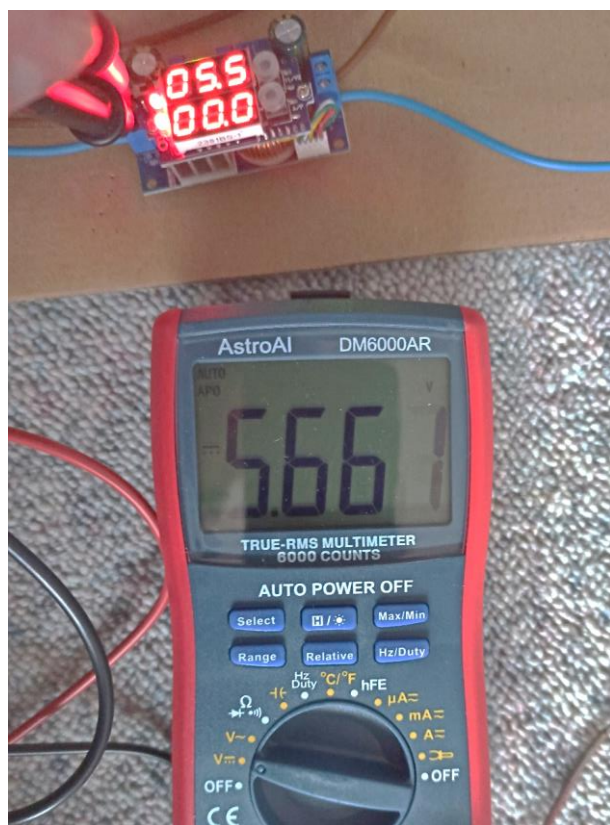


Figure 28. Output voltage of TEG.

## 5 POTENTIAL THERMOELECTRIC GENERATOR SETUP FOR A KILN

CTB ceramic technology GmbH Berlin has designed and produced variety of different kilns. They can be very small with a size of 1 m<sup>3</sup> up to really large size of around 800 m<sup>3</sup>. The heating can be done electrically or with natural gas. Also, a combination of both, so-called hybrid kiln, is possible. The unique design of CTB's own developed burners is the possibility of handling, besides natural gas, also different gases such as hydrogen or wood gas. CTB's designed kilns are highly sophisticated and the energy consumption is economically well-balanced.

Most kilns designed by CTB ceramic technology GmbH Berlin are built with an outer steel shell which is inside coated with a high temperature insulation wool. This insulation wool is suitable for ultra-light refractory solutions in application fields where temperatures of up to 1650 °C can be achieved. For higher temperatures up to 1800 °C it is necessary to build the kiln with bricks.

To integrate thermoelectric generators into the kiln system there are several possibilities. As stated in Chapter 3 the thermoelectric generators, depending on the material, have an efficiency of about one to five percent and can be used for direct electricity generation where waste heat is occurring in various industrial and IT processes without extracting too much heat from the flue gas that there is no more draft in the exhaust stack.

### 5.1 Reference Kiln

To have more concrete consideration of a TEG design on a kiln a reference kiln was chosen. Due to the company's policies, where the kiln is located, a picture cannot be published. But a similar, smaller version of the kiln is shown in Appendix 6, which shows the cover picture of the cfi, ceramic forum international magazine, edition 6-7/2018. Here is some technical data of the kiln. The dimensions are approximately as follows: length = 23220 mm, width = 5940 mm, height = 4570 mm. The kiln is equipped with 52 burners with a total power of 16640 kW and the rated operating temperature is 1450 °C. The kiln is a bell kiln, which is moving up to load the products. It has 4 lifting posts, each handling a capacity of 400 kN. The load capacity is 54000 kg. To deal with the volatile organic compounds (VOC) coming out of the ceramic products during the firing process the kiln has a Thermal oxidizer with 4 burners for the post-combustion of these organic substances.

Two heat exchangers are installed into the flue gas channel between TO-Chamber and vent stack. With the help of these heat exchangers, it is possible to recover part of the thermal energy from the exhaust gas for Kiln operation and to increase economic efficiency. The kiln is also equipped with a flue gas cleaning system, which is provided by a different vendor.

The thermoelectric generators can be directly mounted to the outer shell of the combustion chamber or hearth itself. Most kilns designed by CTB ceramic technology GmbH Berlin are built with an outer steel shell which is inside coated with a high temperature insulation wool. This insulation wool is suitable for ultra-light refractory solutions in application fields where temperatures of up to 1650 °C must be achieved. With a temperature around 60 °C of the outer shell during the firing process this solution is not efficient since the so called "cold side" of the TEG can be cooled down to max

30 °C with significant effort to build a forced cooling. Even if it would be possible thermoelectric generators operating at this temperature not efficient, as seen in Equation (2) such small temperature difference  $\Delta T$  between the hot and cold side of the TEG results in a small thermoelectric voltage.

The low temperature of the outer shell of the kiln could be increased by reducing the thickness of the high temperature insulation wool and thus get a higher heat conduction towards the outer shell of the kiln. This in turn puts more thermal stress to the steel of the outer kiln shell. Which is especially a problem of periodic kilns, where for one, the temperature during the firing process is changing and then, of course while loading and unloading the kiln, needs to be cooled down. Additionally, the higher temperature of the outer shell can cause problems to the controlling and measuring instruments located near the kiln shell. Also, special cables need to be used with higher temperature resistance. Not to forget the danger of hazard to the operating personal.

Another place to position the thermoelectric generators is the exhaust duct. Here are the conditions similar to the kiln. The temperature level of the outer shell of the exhaust duct is about the same as for the kiln. The exhaust duct is not surrounded with too many instruments. This leaves more room for the cooling equipment. However, cooling of the TEG's convectional will not have a significant effect, even with large heat sinks. To achieve a good cooling of the cold side a combination of heat sinks and ventilators should be used. This in turn would consume some of the produced electricity, which in turn reduces, depending on how much forced cooling is needed, the overall efficiency of the thermoelectric generator significantly.

The third place where the TEGs can be placed is the exhaust stack. This is the best option since it is placed outside the building, which means it is relatively easy to be shielded. The danger of hazardous contact is minimized. Also, the exhaust stack has a large area, which can be covered with Peltier elements. Additionally, the shape and height of the exhaust stack increases the natural convection of the cooling elements due to the stack effect, as explained in Chapter 4.1.1.

## 5.2 Forced cooling of Peltier elements

Besides the convectional cooling and the cooling with ventilators there are other options to consider. Usually, the kiln is equipped with cooling fans for controlling the temperature of the exhaust gas as well as adjusting the product of combustion (POC). There might be a possibility to use part of these systems for cooling the cold side of the Peltier elements.

The reference kiln has a significant amount of electrical distribution cabinets, which are connected to a water cooling system. The same system could also be used for cooling the Peltier elements.

Both of these two options above require a significant amount of piping either for the air or the water. This would lead to an enormous additional design and construction effort, which in turn would make the installation of a TEG inefficient.

### 5.3 TEG Outline

As the decision was made to install the thermoelectric generator at the exhaust stack, the next question was how to make the design. The original exhaust stack has a round shape with a diameter of 2700 mm. The height is 30,5 m and made of stainless steel. In about 17 m height is a platform for measuring devices, which monitor the polluted exhaust gas. The flue gas does enter the exhaust stack from the side. The height of the upper limit of the entry duct is 4765 mm. The upraining flue gas will not heat up the wall of the exhaust stack right at this height. Figure 29 shows an extraction of the exhaust stack drawing.

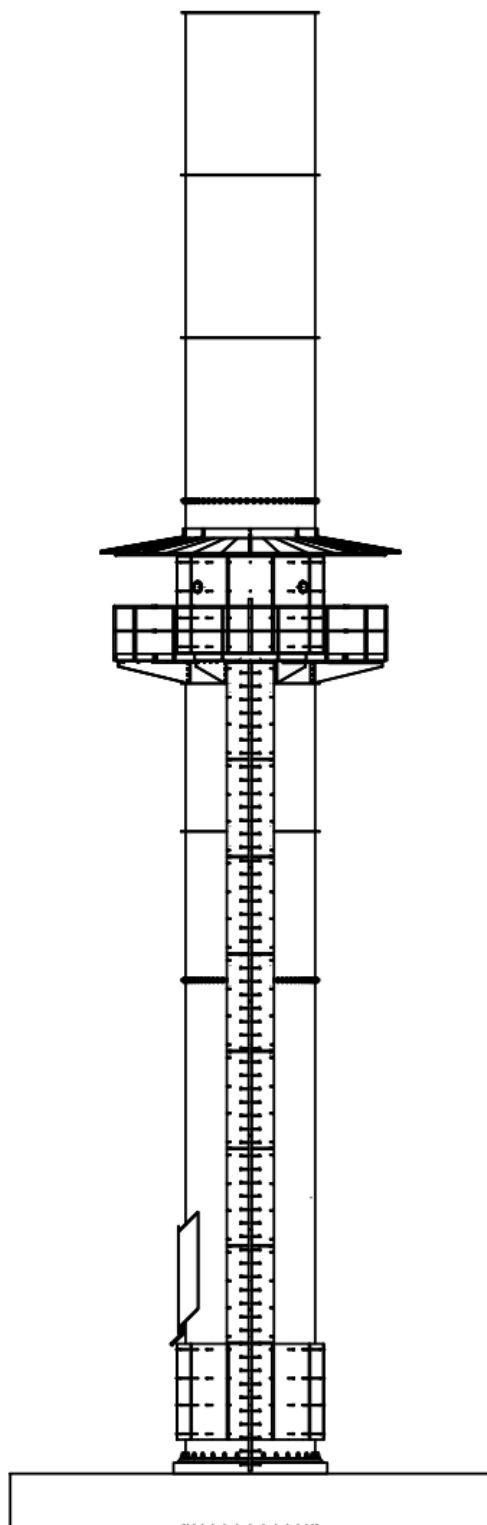


Figure 29. Exhaust stack. (CTB, 2022)

Assuming the exhaust stack has in a height of around 8 m reached the right temperature and subtracting the space needed for the measuring platform the area which can be used for mounting Peltier elements is based on Equation (27) roughly 161 m<sup>2</sup>.

$$A = 2 * \pi * r * h = 2 * \pi * 1,35 \text{ m} * 19 \text{ m} = 161,16 \text{ m}^2 \quad (27)$$

where,

$r$  = radius of the exhaust stack

$h$  = usable height for mounting Peltier elements

There are curved and flexible Peltier elements available, but these are much more expensive than standard flat ceramic coated Peltier elements. Therefore, the exhaust stack should be redesigned with a rectangle shape. Figure 30 shows a simplified sketch of such exhaust stack with the same height of 30,5 m. To have the same volume as the round shaped exhaust stack, the sides should have a width of 2,12 m ( $(2 \cdot \pi \cdot 1,35 \text{ m})/4$ ).

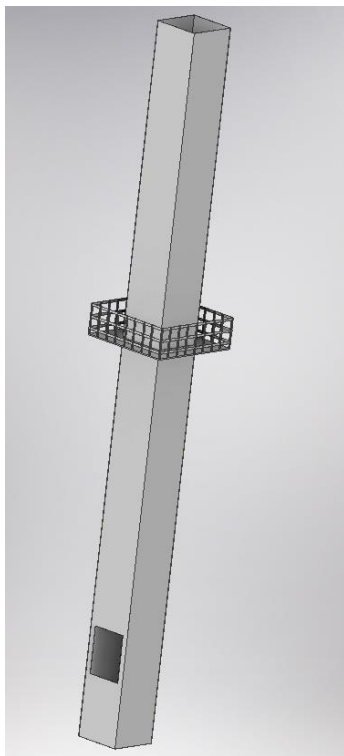


Figure 30. rectangle shaped exhaust stack.

### 5.3.1 Choice of TEG module

TEGs are available for a wide variety of applications and specifications. Simple modules for hobby use are available as well as modules for special applications in the high temperature range. There are TEG manufacturers which are specialized in meeting different requirements, such as high operating temperatures, good fatigue strength or particularly high performance. For the use on the exhaust stack, the choice of TEG modules should be coordinated together with the manufacturer in

order to make the appropriate selection or even initiate a new development for this special application.

The flue gas entering the exhaust stack has a temperature of 329 °C. This is the present situation for the flue gas. The exhaust stack is equipped with an exhaust cooling air valve, which is located at the bottom of the exhaust stack, to adjust the temperature of the exhaust gas released into the atmosphere. When implementing TEG to the system adjustment to temperature management need to be done. A positive effect is that, due to reduced use of the cooling fan, additional energy savings occur, which can be significant considering that the exhaust fan has a power of 25 kW.

Standard Peltier elements can handle temperatures up to 200 °C. The way they are mounted to the exhaust stack should be as easy as possible, to reduce installation costs and for later maintenance. A defect Peltier element should be relatively easily replaceable. A solution to have easy mounting of the Peltier elements and dealing with the allowed maximum temperature the exhaust stack should have a double wall. The heat transfer through air between the inner and outer shell of the exhaust stack will reduce the temperature to fit the Peltier elements requirements. The outer shell will be equipped either with hole or bolts to hold the Peltier elements together with the heat sinks in place, as shown in Figure 31. This means the Peltier elements and heat sinks need to have a hole in the middle, like in Figure 32. For Peltier elements this is not a problem since they are widely available. The heat sinks must be nevertheless ordered customized to meet the necessary cooling capacity to have a sufficient temperature difference  $\Delta T$ .

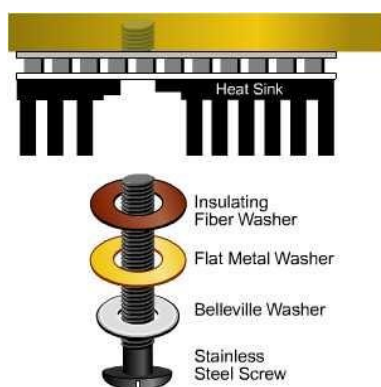


Figure 31. Fastening of TEG. (Ferrotec, 2022)

The choice of the Peltier elements is quite challenging. There are many retailers and manufacturing companies. Some of them are listed in Appendix 3. Often it is very difficult to find detailed information about their products.

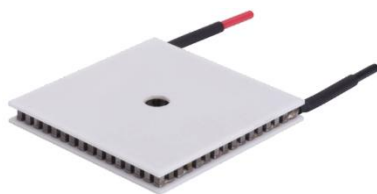


Figure 32. Peltier element with centered hole. (Laird Thermal Systems, 2021)

The chosen Peltier element is presented in Appendix 4. It is available at Eureka Messtechnik Ltd, ([www.eureka.de](http://www.eureka.de)). It is a high temperature Peltier element. This element provides a higher operating temperature and can therefore be used in applications with higher ambient temperatures. The size is 50 mm x 50 mm, which is a little larger than the usual size, which means less mounting work and fewer electrical connections need to be made. Based on the values in Table 4, which are obtained from Appendix 4 and the calculation according to Equation (19) the heat flux going through the Peltier element is 190,28 W.

Table 4. Thermal and electrical data of Peltier element.

symbol	description	value
$\alpha$	Seebeck- coefficient of the TEG	0,0516 V/K
$\beta_{wl}$	Thermal conductivity of the TEG	1,9 W/K
$R_i = R_a$	Internal resistance of the TEG and load resistance on the TEG	0,673 $\Omega$
$T_{max}$	maximum operating temperature	200 $^{\circ}\text{C}$
$\Delta T_{max}$	maximum temperature difference	67,9 K

$$Q_{in} = \frac{1}{2} * 0,673 \Omega * \left( \frac{0,0516 \frac{\text{V}}{\text{K}} * 67,9 \text{ K}}{0,673 \Omega + 0,673 \Omega} \right)^2 - \frac{\left( 0,0516 \frac{\text{V}}{\text{K}} \right)^2 * 473,15 \text{ K} * 67,9 \text{ K}}{0,673 \Omega + 0,673 \Omega} - 1,9 \frac{\text{W}}{\text{K}} * 67,9 \text{ K} = 190,28 \text{ W} \quad (28)$$

Thereafter, the heat flow to be dissipated is calculated according to Equation (21). The calculation results in a heat flow of 185,72 W to be dissipated. The electrical power of the module for these marginal data is calculated based on Equation (15) and has a value of 4,56 W.

$$Q_{out} = \frac{1}{2} * 0,673 \Omega * \left( \frac{0,0516 \frac{\text{V}}{\text{K}} * 67,9 \text{ K}}{0,673 \Omega + 0,673 \Omega} \right)^2 + \frac{\left( 0,0516 \frac{\text{V}}{\text{K}} \right)^2 * 405,25 \text{ K} * 67,9 \text{ K}}{0,673 \Omega + 0,673 \Omega} + 1,9 \frac{\text{W}}{\text{K}} * 67,9 \text{ K} = 185,72 \text{ W} \quad (29)$$

The electrical power of the Peltier element for these marginal data is 4,56 W, which is calculated based on Equation (15).

$$P_{el} = 0,673 \Omega * \left( \frac{0,0516 \frac{V}{K} * 67,9 K}{0,673 \Omega + 0,673 \Omega} \right)^2 = 4,56 W \quad (30)$$

Having now the value for the electrical output of the Peltier the efficiency can be calculated as described in chapter 3.10. According to Equation (22) dividing the 4,56 W for the electrical output of the Peltier element by the 185,72 W for the heat flow, which needs to be dissipated, lead to an efficiency of 2,4 %.

### 5.3.2 Heat sink dimensioning

Determining the actual correct size of a heat sink requires careful design and complicated calculations. To get a good estimate a simplified method was applied. Known from the experiment, the heat sink needs to be rather large if only natural convection is used for cooling. To have an idea of how big the heat sink should be, an estimate of the overall volume of the heat sink required to cool down the Peltier elements was done using following Equation:

$$V = \frac{(Q * Rv)}{\Delta T} = \frac{(185,72 W * 500 \frac{K}{W})}{84,1 K} = 1104 \text{ cm}^3 \quad (31)$$

$\Delta T$  results from the temperature at the cold side of the Peltier element, and the ambient air, which is set to 48 K for this calculation. This temperature is an estimate based on of the heat radiated from the exhaust stack in combination with the average annual temperature of 15,7 °C (TravelChinaGuide, 2022). The value for the Volumetric Thermal resistance of the air (Rv) can be obtained from Table 5, from which the value for natural convection was chosen 500, since due to the stack effect a lower volumetric thermal resistance of the air can be expected.

Table 5. Volumetric Thermal resistance of air. (Celsia, 2022)

air flow	properties	Volumetric Thermal resistance
natural convection	little to no air, no noise	Rv = 500 -800
1,0 m/s	gentle air, low noise	Rv = 150 - 250
2,5 m/s	moderate air	Rv = 80 -150
5,0 m/s	fast, loud air	Rv = 50 -80

A first estimate was done by considering an extruded heat sink with the same size as the Peltier element (50 mm x 50 mm) where the length of the fins is set to be 300 mm. This would lead to a volume of 750 cm<sup>3</sup> (5 cm x 5 cm x 30 cm), which is not quite enough. Increasing one side by 2,2 cm (5 cm x 7,2 cm x 30 cm) gives a better result of 1080 cm<sup>3</sup>.

In a planar fin heat sink, optimum fin spacing is strongly related to two parameters: flow velocity and fin length in the direction of the flow. Table 6 may be used as a guide for determining the optimum fin spacing of a planar fin heat sink in typical applications. (Lee S. , 2022)

Table 6. Fin Spacing versus Flow and Fin Length. (Lee S. , 2022)

flow condition	fin length [mm]			
	75	150	225	300
natural convection	6,5	7,5	10	13
1,0 m/s	4	5	6	7
2,5 m/s	2,5	3,3	4	5
5,0 m/s	2	2,5	3	3,5

The average performance of a typical heat sink is linearly proportional to the width of the heat sink in the direction perpendicular to the flow, and approximately proportional to the square root of the fin length in the direction parallel to the flow. For example, an increase in the width of a heat sink by a factor of two would increase the heat dissipation capability by a factor of two, whereas an increase in the length of the heat sink by a factor of two would only increase the heat dissipation capability by a factor of 1.4. Therefore, if the choice is available, it is beneficial to increase the width of a heat sink rather than the length of the heat sink. Also, the effect of radiation heat transfer is very important in natural convection, as it can be responsible for up to 25% of the total heat dissipation. (Lee S. , 2022)

Under normal conditions the increase of the heat sink in width would apply. In this case it is not suitable for two reasons. The greater the width of the heat sink is, less can be placed in horizontal alignment. The other reason is, through the vertical air flow the dissipated heat from the heat sink will increase the temperature of the air. It means the higher it gets the higher the temperature of the air flowing through the heat sink will be.

Knowing from the calculation for volumetric thermal resistance of the heat sink, the size of the heat sink is roughly 50 mm x 72 mm x 300 mm. This should be the size for dissipation of the heat from the Peltier element to the ambient air with the help of natural convection. With help of the Equation below the dissipation through convection can be calculated.

$$Q = a_c * A * \Delta T \quad (32)$$

where,

$a_c$  = convective heat transfer coefficient

$A$  = surface area

The transfer coefficient consists additive of a convective part  $\alpha_c$  and a radiation. based part  $\alpha_r$ . The convective part is determined by the flow conditions of the surface from the cooling component. The radiation part in turn is dependent on the long-wave, infrared wavelength range emission number and the temperature of the partner with which the component surface is in radiation exchange. (Deutsche Gesellschaft Feuerfest. und Schornsteinbau e.V., 1990)

Without going into complicated calculation methods, such as the similarity theory, simple practical heat transfer calculation and general formula for determining the heat transfer coefficient is given by the following Equation: (Deutsche Gesellschaft Feuerfest. und Schornsteinbau e.V., 1990)

$$\alpha_c = 1,40 \sqrt[4]{\frac{\Delta T_w}{h}} \quad (33)$$

where,

$\Delta T_w$  = temperature difference between surface and air

$h$  = height of heat sink

Having decided a height for the fins of 292 mm for the heat sink, the calculated value for the convective heat transfer coefficient is 5,77 W/m<sup>2</sup>K. The missing 8 mm is the base of the heat sink. This value can now be placed in Equation (32). The Area is calculated based on the dimension of one fin (0,072 m x 0,292 m = 0,021024 m<sup>2</sup>).

$$Q = 5,77 \frac{\text{W}}{\text{m}^2\text{K}} * 0,021024 \text{ m}^2 * 84,1 \text{ K} = 10,2 \text{ W} \quad (34)$$

The amount of 10,2 W for one fin can now be projected to the complete surface of all fins together of the heat sink, like shown in Appendix 5. The surface of one heat sink is 0,4 m<sup>2</sup> and the calculated amount of heat dissipated through the air flowing through the heat sinks is 185,88 W, almost equal to the amount obtained in Equation (29).

### 5.3.3 Electrical output power

Getting back to the available area of the exhaust stack with a width of 2,12 m. Here, 36 Peltier elements can be placed in rows (36 x 0,05 m = 1,8 m), leaving enough space for the electrical connection. The height available for mounting the Peltier elements is 19 m. This means that 263 elements can be placed vertically (263 x 0,072 m = 18,9 m). This leads to an amount of 9468 elements on just one side of the exhaust stack. In total 37872 Peltier elements can be placed on the exhaust stack. Multiplying this by the produced electrical power of one Peltier element of 4,5W, calculated in Equation (30) gives a total electrical output power of 172,7 kW.

### 5.4 Costs analyzes

The prices for Peltier elements vary dependent on design, quality and of course the amount which is purchased. The price for a Peltier element as selected above is about 33 EUR according to vendor Quick-Cool when ordering a minimum of 300 (Quick-Cool 3, 2022). When ordering the amount of 37872 this price can probably be reduced to 25 EUR per element. Having a total price for the Peltier elements of 946800 EUR. Adding to this the heat sink with a price of 10 EUR per piece makes another 378720 EUR. The Peltier elements need to be electrically connected to each other and to a distribution system to feed it, for example, to the power grid of the facility. This requires additional equipment, such as an inverter and distribution cabinets which hold the control systems. All the small materials such as screws and washers should not be forgotten. To calculate the exact amount is out of the scope of this paper. A rough estimate of an additional 200000 EUR is made. Adding the

numbers together gives a total of 1525520 EUR for the needed material. Dividing this by the output power of the TEG system results in an investment of 8833 EUR / kW, excluding installation cost, servicing, maintenance, insurance, return on capital and overhead.

As already mentioned, the kiln is a periodic kiln. One firing cycle takes about 64-68 hours. The kiln runs roughly 120 firing cycles per year. To make the calculation not too complicated it is assumed that the kiln is running 7500 hours per year with an expected lifetime of 10 years, which is a strong understatement, the conceived thermoelectric generator system would produce 12,95 TWh over this period of time. With an investment of 8833 EUR for every produced kilowatt of electrical energy and a total running time of 75000 hours the calculated investment costs for the electrical energy production would be 0,12 EUR / kWh. This is a competitive price despite the high investment costs, at least compared to the current prices for electrical energy in Germany.

## 6 DISCUSSION

The subject of his paper was to investigate the use of thermoelectric generators in industrial kilns to harvest the waste heat and convert it into electrical energy. The use of waste heat is an essential part to the contribution to the reduction of global warming. Making use of waste heat, as it is produced by the exhaust gas from a kiln needs additional investments, which cannot always be economically justified in terms of return of that investment. Therefore, careful considerations must be made when implementing systems, which can make economically reasonable use of waste heat. Heat exchangers have been implemented widely, where the heat is transferred from the hot gas to another gaseous, or liquid medium such as water through conduction.

Thermoelectric generators convert heat energy directly into electric energy. More precise, the difference in temperature across the thermoelectric generator creates a potential difference, which forms a DC Voltage output. Although thermoelectric generators have been in use for over 50 years they have not come into wide use. Mostly because of the low efficiency, which makes them not suitable for energy production. Nevertheless, their advantages as described in Chapter 3 and that fact that the needed input energy is, so to say, for free available makes the production of electrical energy with thermoelectric generators worth while considering, which has been proven by this paper.

The theoretical background of thermoelectric generator was widely explained, which appeared to be necessary since, even so the technical working principle of TEGs is quite simple, the application is rather complex. Not only the production but also the implementation of thermoelectric generators is a challenging task. The considerations for a potential implementation of TEGs into a kiln showed that it should be as best already considered during the early kiln design.

The paper has shown that with present available thermoelectric generators it is possible to accomplish a competitive electrical energy production, despite the low efficiency of this system. As there is ongoing research the price for thermoelectric generators will decrease while the efficiency will increase, making the technology a realistic contributor to the mix of electrical energy production. The implementation design could also be improved by adding to the convectional cooling water cooling. This would have an additional benefit that water heated by the thermal output of the TEG can be used as well, for example for shower water. For example, the 186 W thermal output power which needs to be dissipated into ambient air could heat up about 2,35 liters of water per hour from 12 to 80 °C, making hot water besides electrical energy.

The experimental setup was unfortunately not as successful as hoped. Nevertheless, it was an important contribution to this research. Seeing such a system in action gave a better understanding about the working principle of thermoelectric generators. It showed well where mistakes can easily be made. Especially the design of the heat transfer out of the TEG to maintain the needed temperature difference in order to work.

The actual implementation of TEG in a kiln requires much research and like in many complex machineries requires ultimately extremely far-sighted know-how to make a precise adaptation of the structure to the prevailing conditions to achieve optimal results.

## REFERENCES

- AMI Environmental. (2022, 01 28). *Stack Effect & Infection Control*. Retrieved 01 28, 2022, from <https://amienvironmental.com/stack-effect-infection-control/>
- Browse Biography. (2010, 06 02). *Thomas Johann Seebeck biography*. Retrieved 02 12, 2022, from [http://www.browsebiography.com/bio-thomas\\_johann\\_seebeck.html](http://www.browsebiography.com/bio-thomas_johann_seebeck.html)
- Celsia. (2022, 02 07). *Heat Sink Size Calculator*. Retrieved 02 07, 2022, from <https://celsiainc.com/resources/calculators/heat-sink-size-calculator/>
- CPP Wind Engineering Consultants. (2022, 01 28). *What is the stack effect?* Retrieved 01 28, 2022, from <https://cppwind.com/stack-effect/>
- CTB. (2022, 02 03). EXHAUST STACK - ASSEMBLY. Berlin.
- Deutsche Gesellschaft Feuerfest. und Schornsteinbau e.V. (1990). *Feuerfestbau*. Essen: Vulkan-Verlag.
- ebay. (2022, 11 08). *Aluminium Kühlkörper*. (ebay) Retrieved 11 08, 2022, from <https://www.ebay.de/itm/123767322445>
- eBay. (2022, 02 02). *Controller DC-DC Step-down*. Retrieved 02 02, 2022, from <https://www.ebay.de/itm/272508315658>
- Electrical 4 U. (2020, 08 31). *Seebeck Effect: What is it?* Retrieved 02 12, 2022, from <https://www.electrical4u.com/seebeck-effect-and-seebeck-coefficient/>
- Electrical for Us*. (2016, 11 30). Retrieved 06 30, 2022, from Seebeck Effect and Seebeck Coefficient: <http://www.sanjaysah.com.np/2016/11/seebeck-effect-and-seebeck-coefficient.html>
- Energy Education. (2022). Retrieved 11 19, 2022, from [https://energyeducation.ca/encyclopedia/Second\\_law\\_of\\_thermodynamics](https://energyeducation.ca/encyclopedia/Second_law_of_thermodynamics)
- EURECA Messtechnik. (2018, 10 30). *Peltierelemente von Eureka*. Retrieved 02 12, 2022, from <https://www.eureca.de/862-0-Peltierelemente-von-Eureka.html>
- Fahrner, W., & Schwertheim, S. (2009). *Semiconductor Thermoelectric Generators*. Zurich: Trans Tech Publications.
- Faraji, A. Y., Date, A., Singh, R., & Akbarzadeh, A. (2014, 12). *Base-load Thermoelectric Power Generation Using Evacuated Tube Solar Collector and Water Storage Tank*. Retrieved 02 12, 2022, from Researchgate: [https://www.researchgate.net/figure/Schematic-of-a-commercial-thermoelectric-generator-module\\_fig1\\_274254828](https://www.researchgate.net/figure/Schematic-of-a-commercial-thermoelectric-generator-module_fig1_274254828)
- Ferrotec. (2022, 02 04). *Thermoelectric Technical Reference*. Retrieved 02 04, 2022, from <https://thermal.ferrotec.com/technology/thermoelectric-reference-guide/thermalref06/>
- Fluke. (2021, 12 22). *Thermocouple Fundamentals*. Retrieved 12 22, 2021, from <https://us.flukecal.com/literature/articles-and-education/temperature-calibration/application-notes/thermocouple-app-notes-s>

- Helmholtz-Zentrum Dresden-Rossendorf. (2010, 10 06). *Ionen als Materialbearbeiter*. Retrieved 07 07, 2021, from <https://www.hzdr.de/db/Cms?pOid=13570&pNid=0>
- Kaufland. (2021, 11 06). *Wärmeleitkleber 10 Gramm*. Retrieved 11 06, 2021, from <https://www.kaufland.de/product/391417845/>
- Laird Thermal Systems . (2020). *Thermoelectric Cooler*. Retrieved 11 19, 2022, from <https://www.mouser.com/pdfDocs/Thermoelectric-cooler-options-5-12-20-2.pdf>
- Laird Thermal Systems. (2021, 01 26). *Annular SH Series Thermoelectric Cooler*. Retrieved 02 04, 2022, from <https://deltron.swiss/wp-content/uploads/2021/01/datasheet-SH14-125-045-L1-EP-W4.5.pdf>
- Lee, H. S. (2010). *Thermal design: heat sinks, thermoelectrics, heat pipes, compact heat exchangers, and solar cells*. Hoboken, N.J. : Wiley.
- Lee, S. (2022, 02 07). *HOW TO SELECT A HEAT SINK*. Retrieved 02 07, 2022, from <https://info.boydcorp.com/hubfs/Thermal/Air-Cooling/Boyd-How-to-Select-a-Heat-Sink.pdf>
- Linseis. (2021, 12 22). *Seebeck coefficient*. Retrieved 12 22, 2021, from <https://www.linseis.com/en/properties/seebeck-coefficient/>
- Matthew, D., & Towey, J. (2010, 10). *Two Ways to Measure Temperature Using Thermocouples Feature Simplicity, Accuracy, and Flexibility*. Retrieved 07 09, 2021, from Analog Dialogue: <https://www.analog.com/en/analog-dialogue/articles/measuring-temp-using-thermocouples.html#>
- Meerstetter Engineering. (2022, 02 03). *Peltier Elements*. Retrieved 02 03, 2022, from <https://www.meerstetter.ch/customer-center/compendium/70-peltier-elements>
- Morrison, K., & Dejene, F. K. (2020, 12 23). *American Physical Society*. Retrieved 02 12, 2022, from Thermal Imaging of the Thomson Effect: <https://physics.aps.org/articles/v13/137>
- NASA. (2020, 12 24). *Power Systems*. Retrieved 12 24, 2020, from <https://rps.nasa.gov/power-and-thermal-systems/power-systems/>
- Ouyang, Z. (2016, 04). *Modelling of segmented high-performance thermoelectric generators with effects of thermal radiation, electrical and thermal contact resistances*. Retrieved 12 10, 2021, from Researchgate: [https://www.researchgate.net/publication/300001195\\_Modelling\\_of\\_segmented\\_high-performance\\_thermoelectric\\_generators\\_with\\_effects\\_of\\_thermal\\_radiation\\_electrical\\_and\\_thermal\\_contact\\_resistances/figures?lo=1](https://www.researchgate.net/publication/300001195_Modelling_of_segmented_high-performance_thermoelectric_generators_with_effects_of_thermal_radiation_electrical_and_thermal_contact_resistances/figures?lo=1)
- Quick-Ohm. (2021, 07 14). *10 Regeln thermoelektrischer Generator*. Retrieved 07 14, 2021, from <https://www.quick-ohm.de/pdf/bibliothek/thermogenerator/10-wichtige-regeln.pdf>
- Quick-Cool 1. (2021, 07 09). *PELTIER-Elemente*. Retrieved 07 09, 2021, from <https://www.waermemanagement.com/peltierelemente/download/Erlaeuterung-zu-Peltierelementen.pdf>
- Quick-Cool 2. (2022, 02 08). *Prinzip der Stromerzeugung mittels thermoelektrischer Generator*. Retrieved 02 08, 2022, from <https://quickcool-shop.de/pdf/bibliothek/thermogenerator/prinzip-der-stromerzeugung.pdf>
- Quick-Cool 3. (2022, 07 08). *Thermogeneratoren*. Retrieved 07 08, 2022, from <https://quickcool-shop.de/k4/TEG>

- quickcool-shop. (2021, 12 22). *Prinzip der Stromerzeugung mittels thermoelektrischer Generator*. Retrieved 12 22, 2021, from <https://quickcool-shop.de/pdf/bibliothek/thermogenerator/prinzip-der-stromzeugung.pdf>
- QUICK-OHM. (2021, 07 07). *Peltierelemente*. Retrieved 07 07, 2021, from <https://www.waermemanagement.com/peltierelemente/peltier-module.html>
- RP-Energie-Lexikon. (2020, 12 24). *Thermoelektrischer Generator*. Retrieved 12 24, 2020, from [https://www.energie-lexikon.info/thermoelektrischer\\_generator.html](https://www.energie-lexikon.info/thermoelektrischer_generator.html)
- Schröter, K. (2008, 10 29). *Grundlagen zur Entwicklung eines thermoelektrischen Generators für Kraftfahrzeuge*. (W. H. Zwickau, Editor) Retrieved 12 20, 2020, from Diploma Thesis: [https://libdoc.fh-zwickau.de/opus4/frontdoor/deliver/index/docId/4204/file/Thermoelektrische\\_Generatoren.pdf](https://libdoc.fh-zwickau.de/opus4/frontdoor/deliver/index/docId/4204/file/Thermoelektrische_Generatoren.pdf)
- ScienceDirect. (2020, 12 24). *A comprehensive review of Thermoelectric Generators: Technologies and common applications*. Retrieved 12 24, 2020, from <https://www.sciencedirect.com/science/article/pii/S2352484719306997#b53>
- ScienceDirect. (2022). *Carnot efficiency*. Retrieved 11 19, 2022, from <https://www.sciencedirect.com/topics/engineering/carnot-efficiency>
- Seebeck, T. J. (1895). *Magnetische Polarisation der Metalle und der Erze durch Temperatur-Differenz*. Leipzig: Arthur Joachim von Oettingen.
- Spektrum.de. (2021, 07 21). *Joulesche Wärme*. Retrieved 07 21, 2021, from <https://www.spektrum.de/lexikon/physik/joulesche-waerme/7684>
- TravelChinaGuide. (2022). *Hefei Weather*. Retrieved 12 01, 2022, from <https://www.travelchinaguide.com/climate/hefei.htm>
- Wärmemanagement. (2021, 07 28). *PELTIER - Elemente*. Retrieved 07 28, 2021, from <https://www.waermemanagement.com/peltierelemente/download/Erlaeuterung-zu-Peltierelementen.pdf>
- Western Michigan University. (2020, 12 23). *Thomson Effect, Exact Solution, and Compatibility Factor*. Retrieved 12 23, 2020, from <http://homepages.wmich.edu/~leehs/ME695/Chapter%205.pdf>
- Zhou, C., Lee, Y.K., Yu, Y. et al. (2021, 08 02). *Polycrystalline SnSe with a thermoelectric figure of merit greater than the single crystal*. Retrieved 01 30, 2022, from Nature: <https://www.nature.com/articles/s41563-021-01064-6>

## Specification of Thermoelectric Module

TEC1-12706

### Description

The 127 couples, 40 mm × 40 mm size single module which is made of our high performance ingot to achieve superior cooling performance and 70°C or larger delta T max, is designed for superior cooling and heating applications. Beyond the standard below, we can design and manufacture the custom made module according to your special requirements.

### Features

- No moving parts, no noise, and solid-state
- Compact structure, small in size, light in weight
- Environmental friendly
- RoHS compliant
- Precise temperature control
- Exceptionally reliable in quality, high performance

### Application

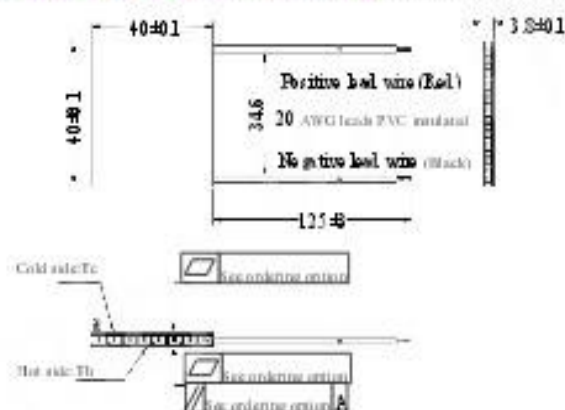
- Food and beverage service refrigerator
- Portable cooler box for cars
- Liquid cooling
- Temperature stabilizer
- CPU cooler and scientific instrument
- Photonic and medical systems

### Performance Specification Sheet

Th(°C)	27	50	Hot side temperature at environment: dry air, N2
DTmax(°C)	70	79	Temperature Difference between cold and hot side of the module when cooling capacity is zero at cold side
Umax(Voltage)	16	17.2	Voltage applied to the module at DTmax
I <sub>max</sub> (amps)	6.1	6.1	DC current through the modules at DTmax
QC <sub>max</sub> (Watts)	61.4	66.7	Cooling capacity at cold side of the module under DT=0 °C
AC resistance(ohms)	1.8~2.2	2.0~2.4	The module resistance is tested under AC

### Geometric Characteristics

Dimensions in millimeters



### Flatness/ Parallelism Option

Suffix	Thickness / H (mm)	Flatness / Parallelism (mm)	Lead wire length (mm) Standard/Optional length
TF	0.3.8±0.1	0:0.05/0.05	125±0.5 specify
TF	1.3.8±0.05	1:0.025/0.025	125±0.5 specify
TF	2.3.8±0.03	2:0.015/0.015	125±0.5 specify

Eg. TF01: Thickness 3.8±0.1(mm) and Flatness 0.025/0.025(mm)

### Manufacturing Options

#### A. Solder:

1. T100: BiSn (Melting Point=138 °C)
2. T200: CuSn (Melting Point= 227 °C)

#### B. Sealant:

1. NS: No sealing (Standard)
2. SS: Silicone sealant
3. EPS: Epoxy sealant
4. Customer specify sealing

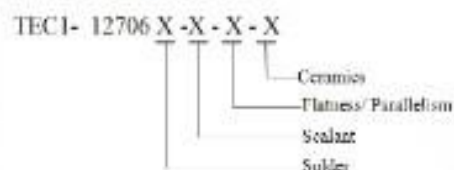
#### C. Ceramics:

1. Alumina (Al<sub>2</sub>O<sub>3</sub>, white 96%)(AIO)
2. Aluminum Nitride (AlN)

#### D. Ceramics Surface Options:

1. Blank ceramics (not metalized)
2. Metalized (Copper-Nickel plating)

### Naming for the Module



TEC1-12706- T100 -NS - TF02 - AIO

T100: Solder, BiSn (Melting Point=138°C)

NS: No sealing

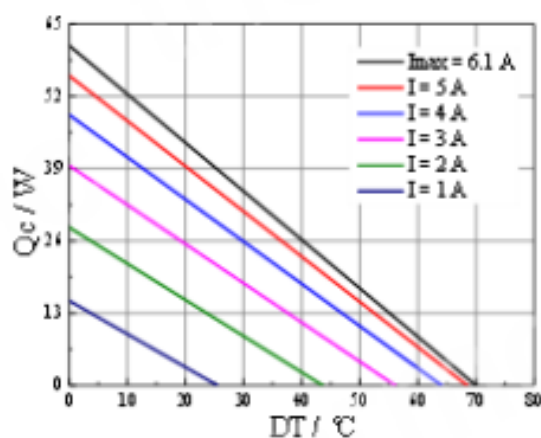
AIO: Alumina white 96%

TF02: Thickness ±0.1(mm) and Flatness/Parallelism 0.015/0.015(mm)

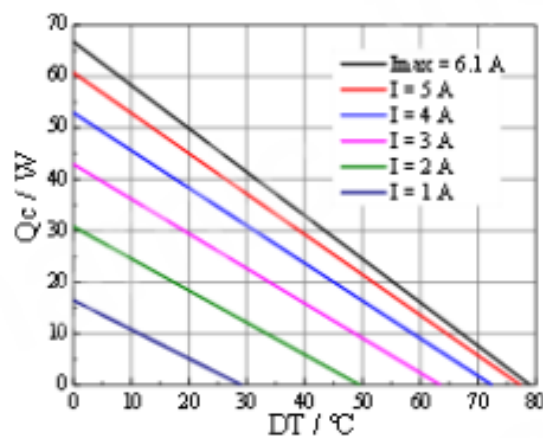
## Specification of Thermoelectric Module

TEC1-12706

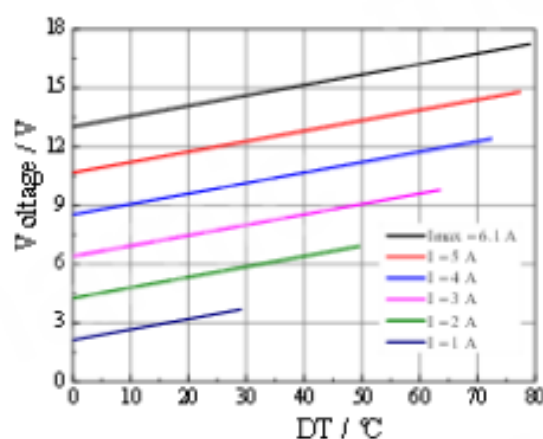
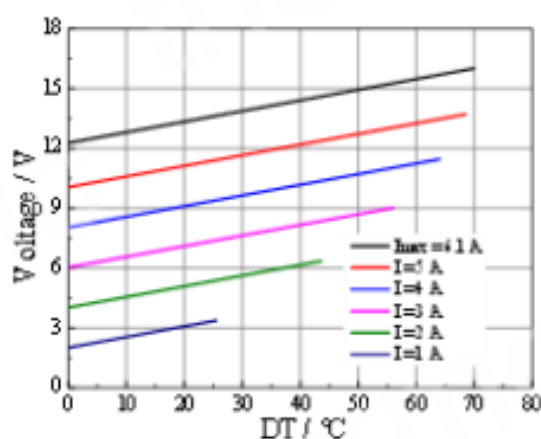
**Performance Curves at  $T_h=27\text{ }^\circ\text{C}$**



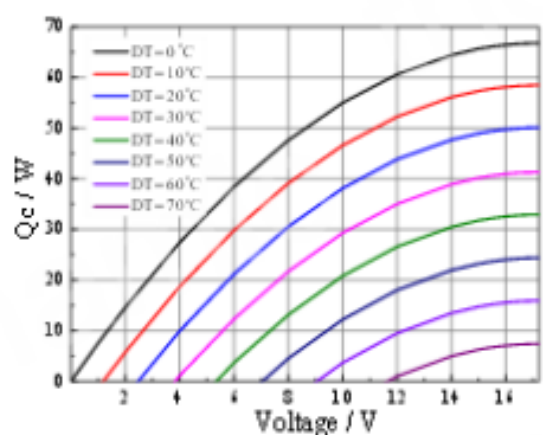
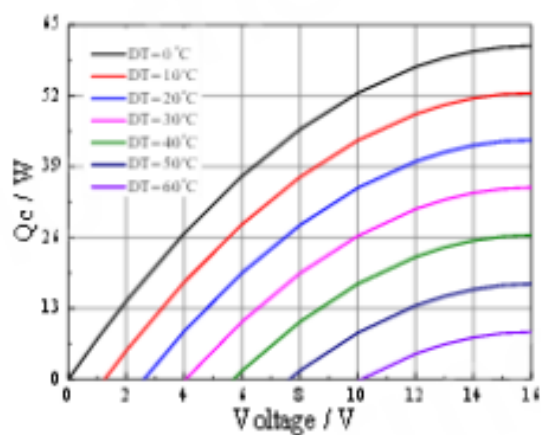
**Performance Curves at  $T_h=50\text{ }^\circ\text{C}$**



Standard Performance Graph  $Q_c = f(DT)$



Standard Performance Graph  $V = f(DT)$

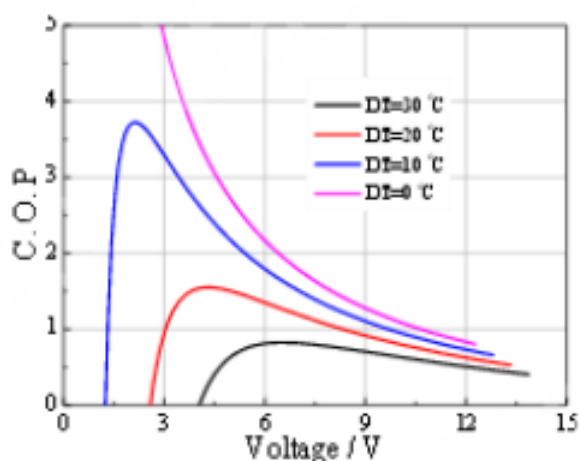


Standard Performance Graph  $Q_c = f(V)$

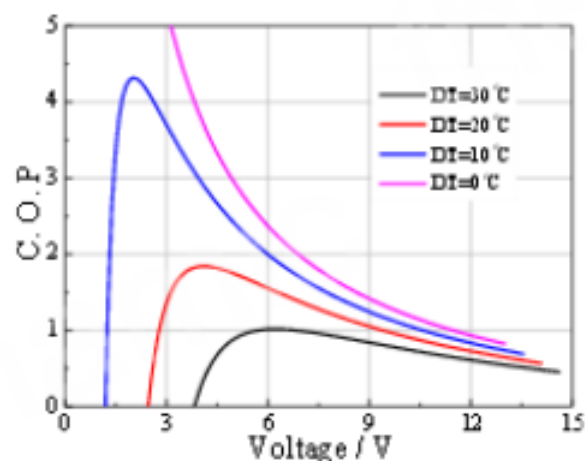
## Specification of Thermoelectric Module

TEC1-12706

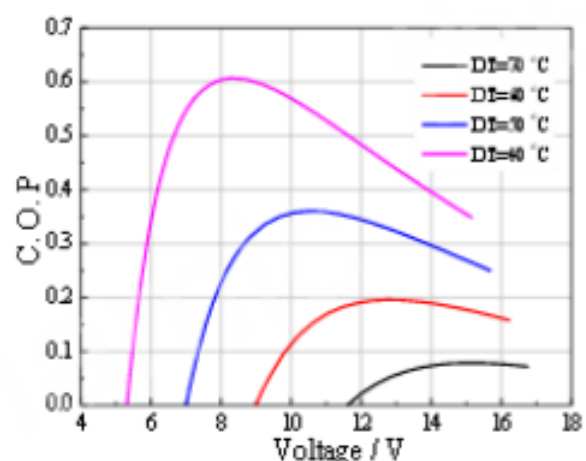
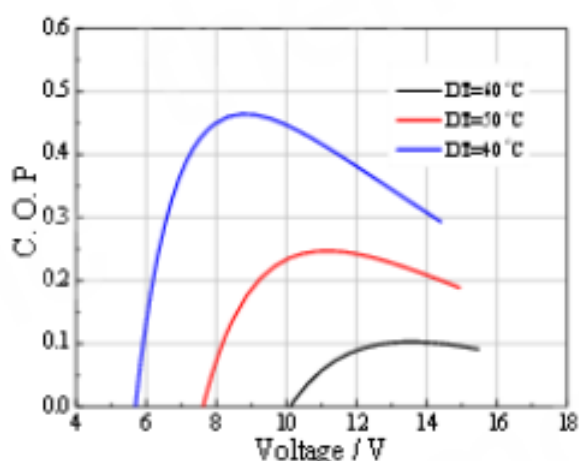
### Performance Curves at $T_h=27\text{ }^\circ\text{C}$



### Performance Curves at $T_h=50\text{ }^\circ\text{C}$



Standard Performance Graph COP = f(V) of  $\Delta T$  ranged from 0 to  $30\text{ }^\circ\text{C}$



Standard Performance Graph COP = f(V) of  $\Delta T$  ranged from 40 to  $60/70\text{ }^\circ\text{C}$

Remark: The coefficient of performance (COP) is the cooling power  $Q_c$ /input power ( $V \times I$ ).

### Operation Cautions

- Cold side of the module sticked on the object being cooled
- Hot side of the module mounted on a heat radiator
- Operation or storage module below  $100\text{ }^\circ\text{C}$
- Operation below  $I_{max}$  or  $V_{max}$
- Work under DC

## APPENDIX 2: DC-DC CONVERTER

## MPPT Solar Panel Controller 5A DC-DC Step-down CC/CV Charging Module LED Display

### Double LED Display



### Product description:

Module Name: 5A buck constant voltage constant current MPPT

Module Properties: Non-isolated buck module (BUCK)

Input voltage: 6-36V

Output voltage:

1.25-32V continuously adjustable (the default output 5V)

MPPT voltage setting range: 6-36V

Output current range: 0.05-5A (The default output current is 3A)

Turn lights output range: 0.01-5A (default turn lamp current 0.3A) the current range will be a little difference because the parts parameter error.

Multifunction double display: input voltage, output voltage, output current, output power

Operating temperature: -40 to + 85 degree

Operating frequency: 180KHz

Conversion efficiency: up to 95% (efficiency, input & output voltage, current and pressure-related)

Short circuit protection: Yes

Over temperature protection: (automatically shut off the output after overtemperature)

Input reverse polarity protection: None, (if necessary, please add the string into the diode)

Output anti-anti-irrigation protection: no, the output must be connected to the battery plus blocking diode, otherwise it will burn the module!

Charging indicator: charging red, bright green when fully charged. Turn lamp is the output current detection.

Installation: 4 pcs 3mm screws

Connection: IN is the input, OUT is output

Module dimensions:60 x 31 x 22 mm (without meter)

### Note:

Detection module, please do not direct connect the output of negative electrode and the input of negative electrode

**Applications:**

- 1, DIY a voltage Regulator, with constant current function, Short-circuit proof, can protect the load.
- 2, It can power supply for electronic devices.
- 3, For a variety of battery charge, can observe the state of charge.
- 4, charger for all kinds of batteries, with MPPT function, can enhance the charging current to double. With a constant current and prevents battery overcharge, effective protection of the battery.
- 5, it can support high-power LED.
- 6, As a car power supply, it can for your cell phone or digital products supply.

**Package Included:**

1PCS \* 5A MPPT Solar Panel Controller DC-DC Step-down CC/CV Charging Module LED Display

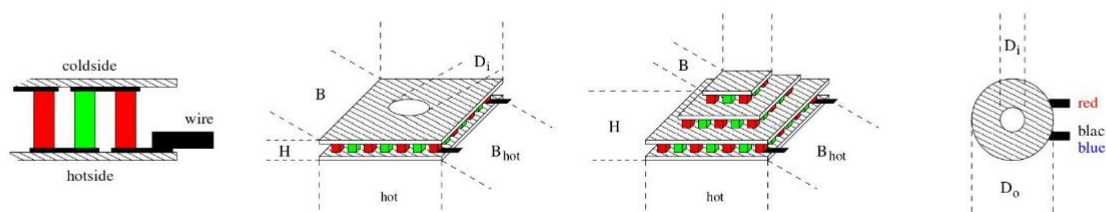
(eBay, 2022)

## APPENDIX 3: PELTIER ELEMENT MANUFACTURES

List of Peltier element manufactures (Meerstetter Engineering, 2022)

<b>Manufacturer</b>	<b>Description</b>	<b>Country</b>
<b>Deltron AG</b> <a href="http://www.deltron.ch">www.deltron.ch</a>	Thermoelectric Modules	Switzerland
<b>Ferrotec</b> <a href="http://www.thermal.ferrotec.com">www.thermal.ferrotec.com</a>	Thermoelectric Modules	USA, Asia, Europe
<b>RMT Ltd.</b> <a href="http://www.rmtltd.ru">www.rmtltd.ru</a>	Miniature to high-performance Peltier elements	Russia
<b>Laird</b> <a href="http://www.lairdthermal.com">www.lairdthermal.com</a>	Thermoelectric Modules	United Kingdom
<b>II-VI</b> <a href="http://www.i-vi.com">www.i-vi.com</a>	Thermoelectric Modules	USA, Asia, Europe
<b>CUI Devices</b> <a href="http://www.cuidevices.com">www.cuidevices.com</a>	Thermoelectric Modules	USA
<b>Kryotherm</b> <a href="http://www.kryothermtec.com">www.kryothermtec.com</a>	Thermoelectric Modules	Russia
<b>Peltron GmbH</b> <a href="http://www.peltier.de">www.peltier.de</a>	Thermoelectric modules, elements for thermocyclation	Germany
<b>Europaan Thermodynamics Ltd</b> <a href="http://www.europaanthermodynamics.com">www.europaanthermodynamics.com</a>	Thermoelectric modules, elements for thermocyclation	Germany

## professional high power peltier element



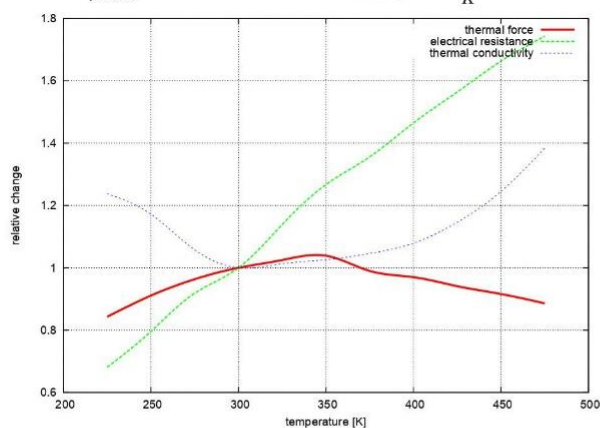
### thermal and electrical data:

thermal force:

resistance:

thermal conductivity:

$\alpha_{300K}$	0.0516	$\frac{V}{K}$
$\rho_{300K}$	0.673	$\Omega$
$\gamma_{300K}$	1.90	$\frac{W}{K}$



available maximum operating temperatures:  $T_{max}$  125, 150, 200, 250 °C  
 tolerances:  $\pm 15\%$

### mechanical data:

size of cold side:

 $L \times B \times H$  50.0 × 50.0 × 3.30 mm

size of hot side:

 $L_{hot} \times B_{hot}$  50.0 × 50.0 mm

height tolerance:

 $\Delta H$   $\pm 0.5$  mm

length and width tolerances:

 $\Delta L$  and  $\Delta B$   $\pm 1.0$  mm

weight:

 $m$  38 g

ceramic plates:

BK-100 (grey), BK-96 (white) or AlN (opaque)

location of production:

China

### experimental data:

typical values at:

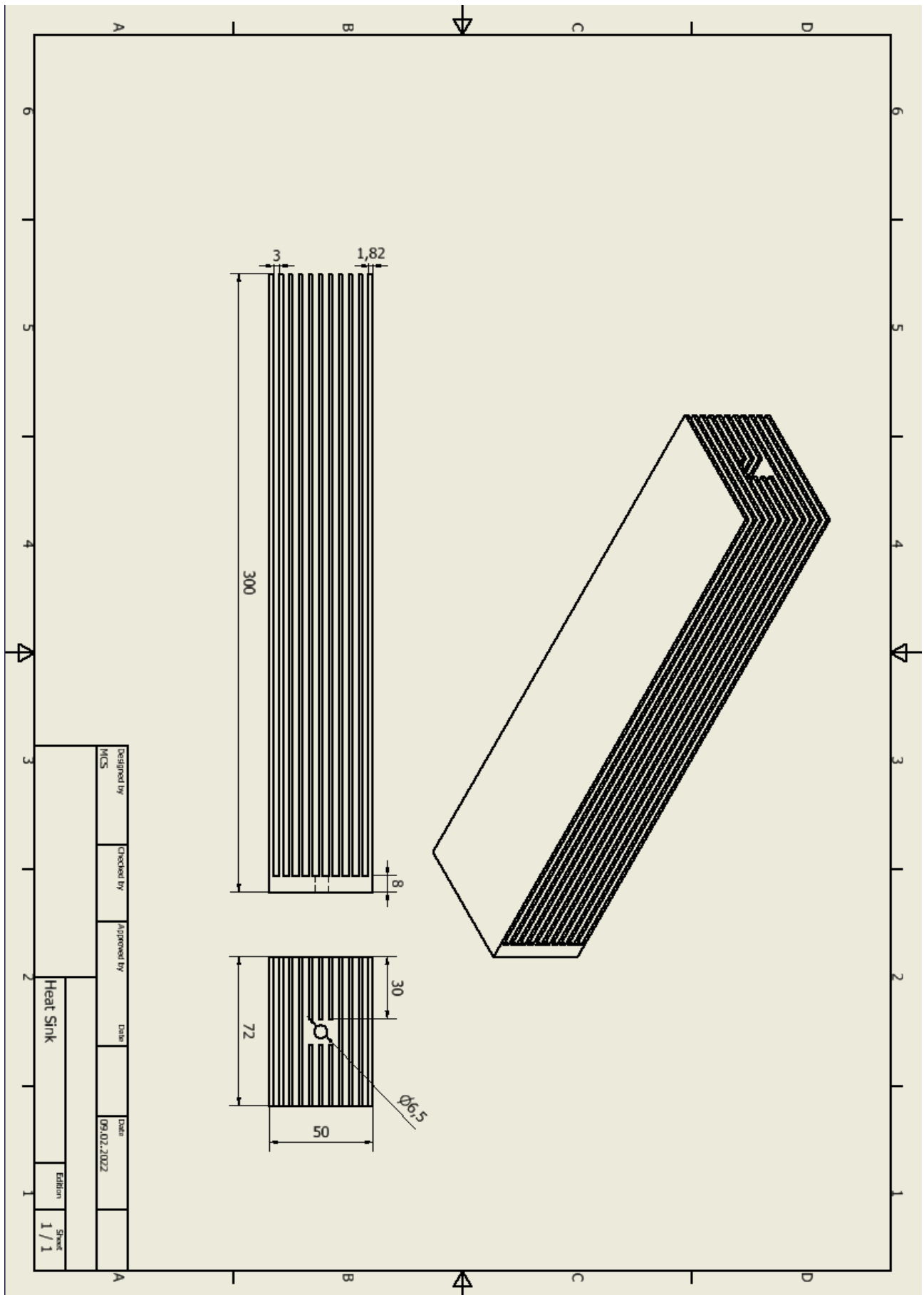
 $T_h = 50^\circ C$ :  $T_h = 300 K$ :

		$T_h = 50^\circ C$ :	$T_h = 300 K$ :
maximum cooling power:	$Q_{max}$	206.6 W	178.0 W
	at $\Delta T = 0$ and $I_{Q_{max}}$	24.8 A	23.0 A
maximum temperature difference:	$\Delta T_{max}$	67.9 K	60.0 K
	at $Q = 0$ and $I_{\Delta T_{max}}$	19.6 A	18.4 A
	$U_{max}$	16.7 V	15.5 V

### order information:

TEC2H-50-50-207/68-CS: sealed, max. 125°C  
 TEC2H-50-50-207/68-DS: sealed, max. 150°C  
 TEC2H-50-50-207/68-HS: sealed, max. 200°C

APPENDIX 5: HAET SINK



## APPENDIX 6: EXAMPLE OF A BELL KILN



Figure 33. Bell Kiln. (CTB, 2022)

Figure 33 shows a Bell kiln build by CTB ceramic technology GmbH Berlin. The picture was published in the magazine cfi, ceramic forum international, edition 6-7/2018.